Great Britain Journals Press

www.journalspress.com

LONDON JOURNAL OF ENGINEERING RESEARCH

Volume 23 | Issue 2 | Compilation 1.0

They were leaders in building the early foundation of modern programming and unveiled the structure of DNA Their work inspired environmental movements and led to the discovery of new genes They've gone to space and back taught us about the natural world dug up the earth and discovered the origins of our species They broke the sound barrier and gender barriers along the way The world of research wouldn't be the same without the pioneering efforts of famous research works made by these women Be inspired by these explorers and early adopters- the women in research who helped to shape our society We invite you to sit with their stories and enter new areas of understanding This list is by no means a complete record of women to whom we are indebted for their research work but here are of history's greatest research contributions made by...

Read complete here:
https://goo.gl/1vQ3lS

Women In Research

Computing in the cloud!

Cloud Computing is computing as a Service and not just as a Product Under Cloud Computing...

Read complete here:
https://goo.gl/VvHC72

Writing great research...

Prepare yourself before you start Before you start writing your paper or you start reading other...

Read complete here:
https://goo.gl/np73jP

Journal Content
In this Issue

Great Britain Journals Press

Editorial Board

Curated board members

Dr. Rocío Maceiras

Associate Professor for Integrated Science,
Defense University Center, Spain Ph.D., Chemical
Engineering, University of Vigo, SPAIN

Dr. Rolando Salgado Estrada

Assistant Professor,
Faculty of Engineering, Campus of Veracruz,
Civil Engineering Department, Ph D.,
Degree, University of Minho, Portugal

Dr. Abbas Moustafa

Department of Civil Engineering,
Associate Professor, Minia University, Egypt, Ph.D
Earthquake Engineering and Structural Safety,
Indian Institute of Science

Dr. Wael Salah

Faculty of Engineering,
Multimedia University Jalan Multimedia,
Cyberjaya, Selangor, Malaysia, Ph.D, Electrical and
Electronic Engineering, Power Electronics and Devices,
University Sians Malaysia

Prof. Baoping Cai

Associate Professor,
China University of Petroleum,
Ph.D Mechanical and Electronic Engineering,
China

Dr. Kao-Shing Hwang

Electrical Engineering Dept.,
Nationalsun-Yat-sen University Ph.D.,
Electrical Engineering and Computer Science,
Taiwan

Dr. Mu-Chun Su

Electronics Engineering,
National Chiao Tung University, Taiwan,
Ph.D. Degrees in Electrical Engineering,
University of Maryland, College Park

Nagy I. Elkalashy

Electrical Engineering Department,
Faculty of Engineering,
Minoufiya University, Egypt

Dr. Vitoantonio Bevilacqua

Department of Electrical and Information
Engineering Ph.D., Electrical Engineering
Polytechnic of Bari, Italy

Prof. Qingjun Liu

Professor, Zhejiang University, Ph.D.,
Biomedical Engineering,
Zhejiang University, China

Research papers and articles

A Table that Produces DNA

Wu Jianxun

ABSTRACT

How does DNA originate, how does DNA come into being, and what are the rules? According to the TongYilogic of "the TongYiLun Thought", combined with the DNA composition mode that has been found now, after determining that the mechanism of increasing yang in DNA system is that the increase of deoxyribose number causes the transformation order of four bases, the differentiation of deoxyribose, phosphoric acid and bases constitutes 128 kinds of basic DNA, thus forming the cycle table of DNA production.

A Table that Produces DNA

Wu Jianxun

ABSTRACT

How does DNA originate, how does DNA come into being, and what are the rules? According to the TongYilogic of "the TongYiLun Thought", combined with the DNA composition mode that has been found now, after determining that the mechanism of increasing yang in DNA system is that the increase of deoxyribose number causes the transformation order of four bases, the differentiation of deoxyribose, phosphoric acid and bases constitutes 128 kinds of basic DNA, thus forming the cycle table of DNA production.

Author: No. 18 Keyuan Road, National New Media Industry Base, Daxing District, Beijing, 102628, China.

The DNA here is extended on the basis of the existing concept, which refers to fragments composed of bases, phosphoric acid and deoxyribose.

So, what is the rules of DNA production? People can get a lot of experimental data and results from experiments, but this is obviously not enough. People need to analyze the experimental results, which is just like "analytical chemistry". People need some logical, mathematical or other tools to analyze, compare or synthesize it, so as to find out the relationship between these experimental results and get the rules of DNA production.

There is a paper that needs to be mentioned and paid attention to, which is *A Table That Produces Elements* published by Wu Jianxun in the American magazine---*Advances in Chemical Engineering and Science* in 2022 (https://www.scirp.org/journal/paperinformation.aspx?paperid=120438. This paper discusses the principle of how elements generate 128 basic elements when they are formed. In the introduction of this paper,

a series of basic theories of philosophy and science are introduced in detail, so I won't go into details here. The key to the success of this paper is that it uses the "TongYi Logic" created by Wang Xijia and Wu Jianxun in the "TongYiLun Thought [2] and Wu Jianxun in *Object, Concept Science and the Essence of Mathematics*" [3] to analyze the production of elements, thus obtaining the rules of the production table of elements. Similarly, we need to use "TongYi Logic" to analyze the production of DNA here, so as to get the cycle table of DNA production or DNA production table.

I. INTRODUCTION

As stated in the above-mentioned paper: "As physics, chemistry and biology, human conceptual science is also developing, that is to say, mathematics, logic and psychology are also developing. On the basis of experimental methods, human beings should also seek more progress in tool science. From Klein's *Ancient and Modern Mathematical Thoughts*[4], we can see that mathematics is developing. Logic, like mathematics, is also developing. From Aristotle's syllogism logic to the development of modern logic and contemporary logic, the development of logic is also fascinating. In logic, Hegel's *Logic* [5] is unique, and Wittgenstein's *Philosophy of Logic* [6] makes an in-depth analysis of logic. As for the development history of logic, Niels' *The Development of Logic* [7] depicts the development course of logic, and China logician Jin Yuelin's simple logic theory *Logic* [8] and Zhu Zhikai's *Logic and Method* [9] also have unique insights. "

"TongYi Logic" is a strict logical science system based on the previous logic and demonstrated by philosophy and science, and it is not a subjective conclusion.

II. QUOTATION OF THE TWELVE SYSTEM LOGIC [10] RULES OF "TONGYI LOGIC" SYSTEM

It is the establishment of unified logic that leads to a new idea of DNA production in biology. That is, DNA has a rules of origin, which is the DNA production table or the DNA production cycle table.

In TongYi's logic, there are twelve system logics that reveal the laws of the generation of things. As long as the conditions comply with the Yin Yang law, BianZheng positive law, and TongYiTi law, they can generate twelve systems. And the DNA system precisely meets this logical condition, so it is a complete generation system of twelve systems.

Twelve System Logic tables are expressed as follows, in which the name of the product in the table is the totlename of its properties:

Table 1: Twelve-System Logic Table

upper hexagra lowest hexagra	坎	坤	震	巽	乾	兑	艮	离
坎（a new system of upper and lower dialectics）	128坎	127师	126解	125涣	124讼	123困	122蒙	121未济
	64离	63同人	62家人	61丰	60明夷	59贲	58革	57既济
坤	120比	119坤	118豫	117观	116否	115萃	114剥	113晋
	56大有	55乾	54小畜	53大壮	52泰	51大畜	50夬	49需
震（a new system of upper and lower dialectics）	112屯	111复	110震	109益	108无妄	107随	106颐	105噬嗑
	48鼎	47姤	46巽	45恒	44升	43蛊	42大过	41井
巽（a new system of upper and lower dialectics）	104井	103升	102恒	101风	100姤	99大过	98蛊	97鼎
	40噬嗑	39无妄	38益	37震	36复	35颐	34随	33屯
乾	96需	95泰	94大壮	93小畜	92乾	91夬	90大畜	89大有
	32晋	31否	30观	29豫	28坤	27剥	26萃	25比
兑	88节	87临	86归妹	85中孚	84履	83兑	82损	81睽
	24旅	23遁	22渐	21小过	20谦	19艮	18咸	17蹇
艮	80蹇	79谦	78小过	77渐	76遁	75咸	74艮	73旅
	16睽硫S	15履磷P	14中孚硅Si	13归妹铝Al	12临镁Mg	11损钠Na	10兑氖Ne	09节氟F
离（a new system of upper and lower dialectics）	72既济	71明夷	70丰	69家人	68同人	67革	66贲	65离
	08未济	07讼	06涣	05解	04师	03蒙	02困	01坎

The relative attributes of yin and yang within the upper and lower 64 hexagrams are as follows:

组别	阳	与阳相对应的阴
坤组	乾、颐、坎、小过	坤、大过、离、中孚
中孚组	屯、蒙、遁、大壮	临、观、革、鼎
离组	需、讼、震、艮	晋、明夷、巽、兑
坎组	师、大有、咸、益	比、同人、恒、损
小过组	小畜、谦、噬嗑、困	履、豫、贲、井
乾组	泰、随、渐、未济	否、蛊、归妹、既济
颐组	复、夬、旅、涣	剥、姤、丰、节
大过组	无妄、大畜、蹇、解	家人、睽、萃、升

According to the ShiErXiTong logic, the above table follows the "ShiErXiTongHouBianZheng logic" and the "ShiErXiTongHouBianZheng TongYi logic ", i.e. Based on (Gan 1+ Gan 2+ Li 1 dialectical Li 2+ Zhen 1 dialectical zhen 2), driven by (Dui 1+ Dui 2+ Gen 1+ Gen 2), and (Kun 1+ Kun 2+ Kan 1 dialectical Kan 2+ Xun 1 Dialectical Xun 2) for leading. The three BianZheng are

A Table that Produces DNA

unified in the "unity" of the total system composed of twelve systems. At the same time, these twelve systems follow the "ShiErXiTong-HouSiXiang logic" and "ShiErXiTongHouWu-Xiang logic" etc.

III. THE CALCULATION PROCESS OF DNA GENERATION PERIODIC TABLE

The analysis process is as follows:

First, the two major contradictions between yin and yang in the production of DNA. yin and yang are the state properties of things, with yin representing passive properties and yang representing active properties. The contradiction between yin and yang is the contradiction between deoxyribose and phosphoric acid, which is the chemical bond connection mode, and the contradiction between deoxyribose and base, which is the chemical bond connection mode. Phosphoric acid is a basic substance, and deoxyribose is a driving factor of the two contradictions. Phosphoric acid and base are connected by chemical bonds, which is also the "yang" factor. That is to say, the chemical bond between deoxyribose and phosphoric acid is yang, while the chemical bond between deoxyribose and base is yin. Thus, these two contradictions are opposite to each other.

Correspondingly, when the yang contradiction drives the DNA basic BianZZheng, it generates the basic form of the yang system, while the yin contradiction generates the basic form of the yin system.

The interaction of these two contradictions will form the basic image of DNA, which constitutes the state mechanism of the positive movement of deoxyribose, which is the four images. The unity of these two contradictions is DNA properties, which is expressed through the sequence of DNA. It realizes the change of image state by the way of deoxyribose rotating four bases, and the performance of this image state is the arrangement order of A, T, C and G. That is to say, these four bases are the four images of DNA.

Second, what is the composition mechanism of the basic form of DNA?

As we known, the mechanism of increasing the yang of atoms in the atomic system is that during the process of increasing protons, electrons construct the properties of an atom through the operation of outer orbits. Similarly, the 128 basic forms of DNA construct a basic DNA properties through the DNA sequence of base operation.

Here, the three elements of DNA form a certain base sequence by forming three nucleotides to complete the production of 128 basic forms of DNA. This can be verified by the correspondence between DNA and protein, that is, the codon of protein is composed of three bases. This is only a function of the basic form. In fact, the same codon may have other functions, which is also proved by experiments.

This mechanism is the differentiation between deoxyribose, phosphate, and base with the increase of deoxyribose, and its effect is unified in the newly formed DNA sequence, which is a form of "unity". Therefore, this order is not a single element of deoxyribose at work, but a unified result of BianZheng. Instead, phosphate, base, and deoxyribose correspond to four elephantine state changes, and form a three element form with each other, that is, each element has four elephantine state changes, thus BianZheng forms a certain three element form. In this way, the combination of the three elements and the four phenomena forms exactly the 64 forms, driven by the changes in the yin and yang states, and forms the 64 forms corresponding to the inside and outside, thus forming the twelve systems and forming the 128 forms.

Specifically, phosphate, base, and deoxyribose form nucleotides, and the four dimensional changes of the four bases of nucleotides are reflected in the three elements, with changes in yin and yang, resulting in the formation of a twelve DNA system, which forms one hundred and twenty-eight basic DNA forms. This nucleotide mechanism is the morphological mechanism of the three elements, which means that during the formation of morphology, it can only be the BianZhang morphological mechanism of three nucleotides linked between the three elements. Therefore, the triad mechanism is

A Table that Produces DNA

necessary and cannot be two nucleotides or three nucleotides. In layman's terms, it is a hexagram in the form of six trigrams, with each adjacent two trigrams forming one image. Such a hexagram can only consist of three such BianZhang forms. Therefore, the triad mechanism is the morphogenetic mechanism of DNA.

There are two mechanisms for the formation of such DNA, namely, two basic contradictory chemical bonds, and two sixty-four basic morphological systems of yin and yang.

These two systems are in the functional structure of DNA. If it is a basic morphological system, it is a double-stranded structure with opposite yin and yang. For the DNA structure of life, it is a double helix structure of yin and yang.

The sequence of DNA also shows the yin and yang of this double helix and double strand. One direction in a DNA molecule is $5'\rightarrow3'$, and the other direction is $3'\rightarrow5'$. Moreover, DNA polymerase in organisms can only catalyze DNA synthesis from the direction of $5'\rightarrow3'$.

The two strands of DNA are divided into yin and yang under the unified properties, and the positive properties is established on the basis of negative. That is to say, the basic form of DNA on the positive chain is defined in the order of its corresponding increase in yang value. The same codon in the two chains actually represents different properties of yin and yang, and they are completely different basic forms of DNA in the unity property of DNA, just like the property differentiation of atomic system. If it must be expressed by codon, it should be the basic form of positive DNA followed by the negative triplet code and the corresponding positive triplet code.

Compared with the atomic properties formed by the mechanism that the electrons in the atomic system run along a certain orbit and suborbital, the "electrons" or "bases" of DNA living bodies are established by using the arrangement order of four bases at three positions where three deoxyriboses are formed. This is the secret of how DNA works.

So it shows that any form of DNA is based on a "triplet" as the basic unit. This "triplet" is a piece of DNA composed of three adjacent nucleotides.

In other words, any DNA is based on "triplet".

Third, what is the unity property of the basic form of DNA? It is the base sequence representing 128 basic genetic properties.

Forth, the functional structure of DNA. This does not refer to the morphology of 128 basic genes, but to the DNA of the functional structure of a living body.

The DNA of any functional structure is a "compound" of basic genes, and RNA is just a product of DNA.

So, what is the structure of DNA? It includes at least three aspects, namely, DNA unity, DNA material form system, DNA movement form system and DNA thought form system.

For a living body, DNA includes the psychological state of all living individuals, and it is distributed in the twelve systems of living body in the functional differentiation of living body. Therefore, all the properties of individual life are reflected in the DNA system. The DNA system here refers to the functional structure of DNA of living individuals.

Because DNA contains all the psychological states of a living individual, it forms the DNA of the twelve major systems corresponding to the twelve major systems of the living individual. Of course, this still needs to be tested through experiments. Here we can make a theoretical prediction that DNA is a unified class set system with all psychological class sets, ultimately associated with the phenotypes generated by BianZZheng of living individuals, thus forming the overall structure of living individuals.

Then, the standard pattern of DNA can be described by conceptual unification. It is expressed by "the cycle table of concept unification".

The fifth is the basic unit level of life based on DNA. At this level, for some non-cellular life, it

A Table that Produces DNA

may be DNA, or RNA's BianZZheng, together with the individual's functional structure, to form a living body. For cellular organisms, prokaryotes directly form functional structures, while eukaryotes undergo cell division, which can form the BianZZheng of cells, thus forming the basic unit of a living organism, forming the "type and type" structure of their own cellular units.Sixth, the image relationship of DNA.

The form of DNA is four bases. So, which one is shaoyang, shaoyin, laoyang and laoyin?

Cipher has two startup codes, namely AUG and GUG. Among these two startup codes, we investigate the most common AUG startup code. This promoter code refers to the codon of mRNA, which is reflected in the code of "nonsense strand" DNA as TAC. That is to say, in the process of DNA deoxyribose and base connection, it is generated in protein. Deoxyribose first shows the combination with T, which reflects the foundation of T's yang, that is to say, T is shaoyang, which is the basis for the increase of yang, and then the opposite base is A, shaoyin, and then C and G, which are opposite to each other. Then, purine and pyrimidine each have a yin and a yang, so C is Taiyin and G is Taiyang.

Their order properties is their unity, so adenine, guanine, unity order, thymine and cytosine constitute the five-element relationship of wood, fire, earth, gold and water.

Seventh, the sequencing of the basic forms of DNA.

The basic form of DNA is a "triplet" sequence, so how is this sequence sorted? If we sort by yang? This can be derived from the following DNA cycle table and is consistent with the existing "triplet" properties.

The six lines in the DNA periodic table can be replaced with corresponding A, T, C, and G to obtain the triplet code. How to replace it? The triad is actually the BianZheng of the three noumenons, namely the BianZheng of material form, motion form, and thinking form. In this way, the upper two lines, the middle two lines, and the lower two lines are respectively symbolic

states. According to the table below, simply substitute it in.

The order is concerned, because the cycle table has already discharged the order, which is known.

What I want to talk about here is the codon of RNA, which is not 128 basic forms. It is a derivative of the basic form of DNA and cannot replace DNA itself. RNA is not qualified to be the basic form of DNA.

太陽 ▬▬ ▬▬ G guanine	少陽 ▬▬ ▬ ▬ T thymine	太陰 ▬ ▬ ▬ ▬ C cytosine	少陰 ▬ ▬ ▬▬ A adenine

The question is the order of DNA triplet the same as that of hexagrams? This is based on the cycle table of the universe. As can be seen from the start code of codon, it corresponds to the first position in the cycle table, that is, the beginning. In this way, it is a hurdle. Then, after conversion, it is found that if the triplet of DNA is based on the upper, middle and lower levels, it is the lower level in front, the upper level and the middle level in the back, so the order of yang of codons should be changed to be consistent with that of hexagrams.

The positions of the last two bases of the triplet can be reversed, so that the order of increasing the yang of the hexagrams is "three hexagrams" (this means that the triplet is regarded as three hexagrams, that is, two adjacent hexagrams form an image, and an image as a whole is regarded as one hexagram.), the order of the first (lower), middle and upper.

There is a question here, that is, is the rules of this codon universal? Yes, we mentioned earlier that the mechanism of DNA morphogenesis is the triplet mechanism.

Eighth, the cycle table of DNA production (abbreviated as DNA cycle table). In the "living body" system, the most basic "shaped" table is the "DNA cycle table".

As we known, DNA is driven by the contradiction between deoxyribose, phosphoric acid and base, that is, the contradiction between deoxyribose and

A Table that Produces DNA

phosphoric acid, and the contradiction between deoxyribose and base, thus forming two internal and external systems of DNA, that is, yin and yang, thus forming two eight systems, and then forming twelve dialectical systems of the two systems.

We give the cycle table of DNA here

According to the unified naming method of the cycle table of the Universe, namely "serial number+hexagram name+basic form", we give these 128 basic forms of genes a unified name: "serial number+hexagram name+gene", for

example, 128 Kan, its name is "128 Kan gene", and another example is 127 Shi, its name is "127 Shi gene". Among them, the names of hexagrams are arranged in the order of upper hexagram, middle hexagram and lower hexagram.

In the table, we use the "triple code". Although the names of the 64 hexagrams are the same, their properties are that the first 64 hexagrams are yang and the last 64 hexagrams are Yin, and their properties are different. The yin-yang mechanism under the same name is completed by DNA unity and appears as double-stranded yin-yang.

Table 2: Cycle Table of DNA Production

upper hexagram / lowest hexagram	kan	kun	zhen	xun	qian	dui	gen	li
kan (a new system of upper and lower dialectics)	128 kan ACT	127 shi CCT	126 xie CTT	125 huan GCT	124 song GTT	123 kun ATT	122 meng TCT	121 weiji TTT
	64 li TGA	63 tongren GGA	62 jiaren GAA	61 feng CGA	60 mingyi CAA	59 bi TAA	58 ge AGA	57 jiji AAA
kun	120 bi ACC	119 kun CCC	118 yu CTC	117 guan GCC	116 pi GTC	115 cui ATC	114 bo TCC	113 jin TTC
	56 dayou TGG	55 qian GGG	54 xiaochu GAG	53 dazhuang CGG	52 tai CAG	51 dachu TAG	50 guai AGG	49 xu AAG
zhen (a new system of upper and lower dialectics)	112 zhen ACA	111 fu CCA	110 zhen CTA	109 yi GCA	108 wuwang	107 sui ATA	106 yi TCA	105 shike
	48 ding TGT	47 you GGT	46 xun CAT	45 heng CGT	44 sheng CAT	43 gu TAT	daguo 42 AGT	jing 41 AAT
xun (a new system of upper and lower dialectics)	jing 104 AAT	103 sheng CAT	102 heng CGT	101 xun CAT	100 you GGT	daguo 99% AGT	98 gu TAT	97 ding TGT
	40 shike TTA	39 wuwang GTA	38 yi GCA	37 zhen CTA	36 fu CCA	35 yi TCA	34 sui ATA	33 zhen ACA
qian	96 xu AAG	95 tai CAG	94 dazhuang CGG	93 xiaochu GAG	92 qian GGG	91 guai AGG	90 dachu TAG	89 dayou TGG
	32 jin TTC	31 pi GTC	30 guan GCC	29 yu CTC	28 kun CCC	27 bo TCC	26 cui ATC	25 bi ACC
dui	jie 88 ACG	87 lin CCG	86 guimei CTG	85 zhongfu GCG	84 lu GTG	83 dui ATG	82 yang TCG	81 kui TTG
	24 lu TGC	23 dun GGC	22 jian GAC	21 xiaoguo GCG	20 qian CAC	19 gen TAC	18 xian AGC	17 jian AAC
gen	80 jian	79 qian	78 xiaoguo	77 jian	76 dun	75 xian	74 gen	73 lu

A Table that Produces DNA

	16 kui TTG	15lu GTG	14 zhongfu GCG	13 guimei CTG	12 lin CCG	11 yang TCG	Ten dui ATG	jie 09 ACG
gen (a new system of upper and lower dialectics)	72 jiji AAA	71 mingyi CAA	70 feng CGA	69 jiaren GAA	68 tongren GGA	67 ge AGA	66 bi TAA	65 li TGA
	08 weiji TTT	07 song GTT	06 huan GCT	05 xie CTT	04 shi CCT	03 meng TCT	02 kun ATT	01 kan ACT

REFERENCES

1. Advances in Chemical Engineering and Science（2022）, Scientific Research Publishing Inc. USA.
2. TongYiLun Thought, founded by Wang Xijia and Wu Jianxun, China.
3. Wu Jianxun (2020), Object and conceptual Science and The essence of Mathematics. CHINA INTERNATIONAL PRESS, BEAVERTON, OREGON USA.
4. Klein, Ancient and Modern Mathematical Thought, Shanghai Science and Technology Press, 1981.
5. Hegel, Logic, Commercial Press, 1976.12.1
6. Wittgenstein, On Logical Philosophy, Commercial Press, February, 1996.
7. Niel, Martha Niel, Development of Logic, Commercial Press, November 1985
8. Jin Yuelin, Logic, China Renmin University Press, April 2010.
9. Zhu Zhikai, Logic and Method, People's Publishing House, 2003.
10. Wu Jianxun (2020), Object and conceptual Science and The essence of Mathematics. CHINA INTERNATIONAL PRESS, BEAVERTON, OREGON USA .
11. Wu Jianxun (2020), Object and conceptual Science and The essence of Mathematics. CHINA INTERNATIONAL PRESS, BEAVERTON, OREGON USA

London Journal of Engineering Research

A Table that Produces DNA

This page is intentionally left blank

Poly Ionic Liquid based Aqueous Two-Phase Extraction Coupled with UV Spectrophotometry for Separation/analysis of Allura Red in Food

Ahmed Bakheet

ABSTRACT

Poly ionic liquid was introduced as aqueous two-phase extraction (ATPE) sorbent accompanied with UV spectrophotometry for Allura red (AR) separation in food samples.

Different parameters, like pH value, adsorption temperature and time, were studied. the preconcentration factor for AR was 27. The linear range, detection limit (DL), correlation coefficient (R) and relative standard deviation (RSD) were found to be 0.10-9.00 µg/mL, 5.2 µg/L, 0.9987 and 3.10% (n=3, c=4.00 µg/mL).

This method was successfully applied for separation/analysis of allura red pigment in food samples with satisfactory results.

Keywords: allura red; poly acid ionic liquid; aqueous two-phase extraction (atpe); uv spectrophotometry.

Classification: DDC Code: 541.33 LCC Code: QD547

Language: English

Poly Ionic Liquid based Aqueous Two-Phase Extraction Coupled with UV Spectrophotometry for Separation/analysis of Allura Red in Food

Ahmed Bakheet

ABSTRACT

Poly ionic liquid was introduced as aqueous two-phase extraction (ATPE) sorbent accompanied with UV spectrophotometry for Allura red (AR) separation in food samples.

Different parameters, like pH value, adsorption temperature and time , were studied. the preconcentration factor for AR was 27. The linear range, detection limit (DL), correlation coefficient (R) and relative standard deviation (RSD) were found to be 0.10-9.00 μg/mL, 5.2 μg/L, 0.9987 and 3.10% (n=3, c=4.00 μg/mL).

This method was successfully applied for separation/analysis of allura red pigment in food samples with satisfactory results.

Keywords: allura red; poly acid ionic liquid; aqueous two-phase extraction (atpe); uv spectrophotometry.

I.   INTRODUCTION

Synthetic colorants are common food additives used in food industry, due to their stable nature, bright colors and low price. Allura red (Fig.1) is one of the eleven synthetic colorants which are allowed to be used within a certain limit in food, such as ice cream, candies, pastries, beverages, jelly and hams [1]. The maximum usage of AR in candies and beverages are 0.3 g/kg and 0.1g/kg, respectively; which are strictly regulated by the hygienic standards for food additives of China.

Excessive use of safety AR as food additives has been questioned, because AR is potentially toxic and carcinogenic, especially harmful to the intellectual development of children[2].

[1]The AR detection methods included high performance liquid chromatography as a separation method [3], UV-vis spectrophotometry[4], differential pulse polarography[5], voltammetry and Fluorescence spectrophotometry. Fluorescence spectrophotometry as detection method has many advantages of lower-cost analysis, easier operation and better accuracy. Therefore, this method was applied for separation of AR in food samples.
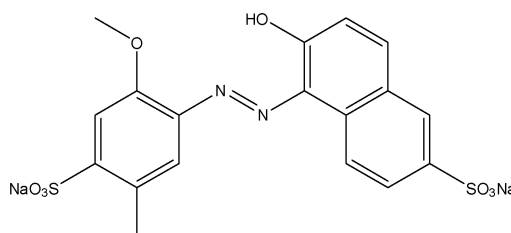
Fig. 1: Chemical Structure of Allura Red

Ionic liquid, also known as low-temperature molten salt, is composed of all ions at room temperature material. Ionic liquids have the advantages of low vapor pressure, good thermal stability, nonflammable and miscible with a variety of solvents. By changing the ionic liquid anion-cation combination or the introduction of functional groups, we can get a large number of functional ionic liquids that can meet the analytical needs and have adjustable performance. Common ionic liquid functionalization methods include 1) improved ionic liquid lipophilicity and surface activity by introduction of long alkyl chains; 2) improved ionic liquid polarity enhancement by incorporation of polar substituents; 3) Hydrogen bond acceptors make ionic liquids and hydrogen bonds stronger; 4) using biomolecules as ionic liquid raw materials

to reduce the toxicity of ionic liquid environment. Ohno's research team successfully prepared a series of amino acid functionalized hydrophilic ionic liquids through ion exchange-neutralization reaction.

Polymerized ionic liquids, poly(ionic liquid)s or polymeric ionic liquids, all abbreviated as PIL is the polymeric form of ionic liquids[6]. They have half of the ionicity of ionic liquids since one ion is fixed as the polymer moiety to form a polymeric chain. PILs have a similar range of applications, comparable with those of ionic liquids but the polymer architecture provides a better chance for controlling the ionic conductivity. They have extended the applications of ionic liquids for designing smart materials or solid electrolytes.

Poly ionic liquid was used in food analysis/separation and enrichment technology used to eliminate the matrix interference and to improve the sensitivity. Common extraction techniques include solid phase extraction and liquid phase extraction. Solid phase extraction was used to load the adsorbent of special materials, and for adsorption and elution of the two processes, the analysis taking a long time, compared with liquid phase extraction, solid phase extraction technology is easier and faster. Liquid phase extraction mainly includes liquid-liquid extraction, single-drop extraction, hollow fiber extraction, dispersion liquid microextraction and aqueous two-phase extraction (ATPE). ATPE is a two-phase system using a two-phase system in a certain concentration, pH, temperature conditions formed by the two-phase extraction and separation technology, compared with the traditional organic solvent extraction, the two-phase system has the advantages of good performance in the biological Compatibility, small interfacial tension, mild operating conditions, adjustable extraction performance and no volatile organic solvent residues, known as green separation technology. The formation of a dual aqueous system [7] includes alcohol-salts, polymers, polymers-polymers, surfactants-salts and the like. Rogers research group [8] for the first time using hydrophilic ionic liquids and K_3PO_4 to form a double aqueous phase. The strong polarity of ionic liquids and ionic liquids larger specific surface area, so that the ionic liquid-based aqueous two-phase extraction is widely used in analytical chemistry [9].

II. EXPERIMENTAL SECTION

2.1 Reagents

All chemicals and reagents were at least of analytical reagent grade, unless otherwise stated. Allura red standards were obtained from the Sigma-Aldrich (Shanghai, China). A standard stock solution was prepared by dissolving 10.0 mg of each standard in 100 mL of ethanol and stored in dark at 4℃. N-methylimidazole (Darui Fine Chemicals, Shanghai, China), 4-chloromethystyrene and 2, 2-Azobis-2 methylpropionitrile (AIBN) were bought from Chemical Reagent Co., Ltd (China). K_3PO_4, N, N-dimethylformamide (DMF), methanol, ethylether, ethyl acetate (Sinopharm Chemical Reagent Co., Ltd., Shanghai, China)

2.2 Equipment

FTIR spectra were measured with a Bruker Tensor 27 spectrometer (Bruker Company, Germany). Samples were pressed into KBr pellets and recorded at the frequencies from 500 to 4500 cm^{-1} with resolution of 4 cm^{-1}. Centrifuge (Anke Scientific Instrument Factory Shanghai,China), timing multifunctional oscillator (Guohua Co., Ltd., China), digital constant temperature water-bath (Guohua Co., Ltd., China).UV-2550 spectrophotometer (Shimadzu Corporation, Japan) was used.

2.3 Preparation of Aqueous Two-Phase Extraction (ATPE) Poly Ionic Liquid (PILs)

2.3.1 Preparation of IL Monomer

1-methylimidazolium IL monomer was prepared through the reaction of 6.56 g of 1-vinylimidazole and 12.21g of 4-chloromethystyrene in 30 mL of methanol at 60℃ for 24 h under vigorous stirring, the product was dried in the vacuum at 50℃ to remove methanol then the product was washed by ethylether (4-5) times and with distilled water 3 times the product was yellow viscous ionic liquid.

Poly Ionic Liquid based Aqueous Two-Phase Extraction Coupled with UV Spectrophotometry for Separation/analysis of Allura Red in Food

10 Volume 23 | Issue 2|Compilation 1.0 © 2023 Great Britain Journals Press

2.3.2 Preparation of Aqueous Two-Phase Extraction (ATPE) Poly Ionic Liquid

0.095g of 2, 2-Azobis-2methylpropionitrile (AIBN) and 15 ml of N, N-dimethylformamide (DMF) were added to the product at 60°C for 24 h.Before the reaction N_2 was inflated to the solution for (20min). The product was poured slowly into a little amount of ethyl acetate then the product was dried in the vacuum for 24 h at 45°C.

2.3.3 Phase Diagram Determination

Amino acid ionic liquids and K_3PO_4 dual aqueous phase using the cloud point method [8] determination, the specific measurement steps are: (1) accurately weighed 0.5000g pure ionic liquid placed in a test tube, the test tube into a water bath, low temperature (2) adding a little water to dissolve the ionic liquid in the test tube and stirring to make the solution clear and transparent; (3) adding saturated K_3PO_4 aqueous solution into the solution until the system just appears When turbidity, record the volume of the inorganic salt solution added; (4) continue to add water dropwise to clarify the cloudy system, and then add saturated K3PO4 aqueous solution to just appear cloudy, record the volume of inorganic salt solution used: Repeatedly and repeatedly calculated the turbidity system ionic liquid and salt mass percentage(Fig.2.), you can get a more complete double junction line.
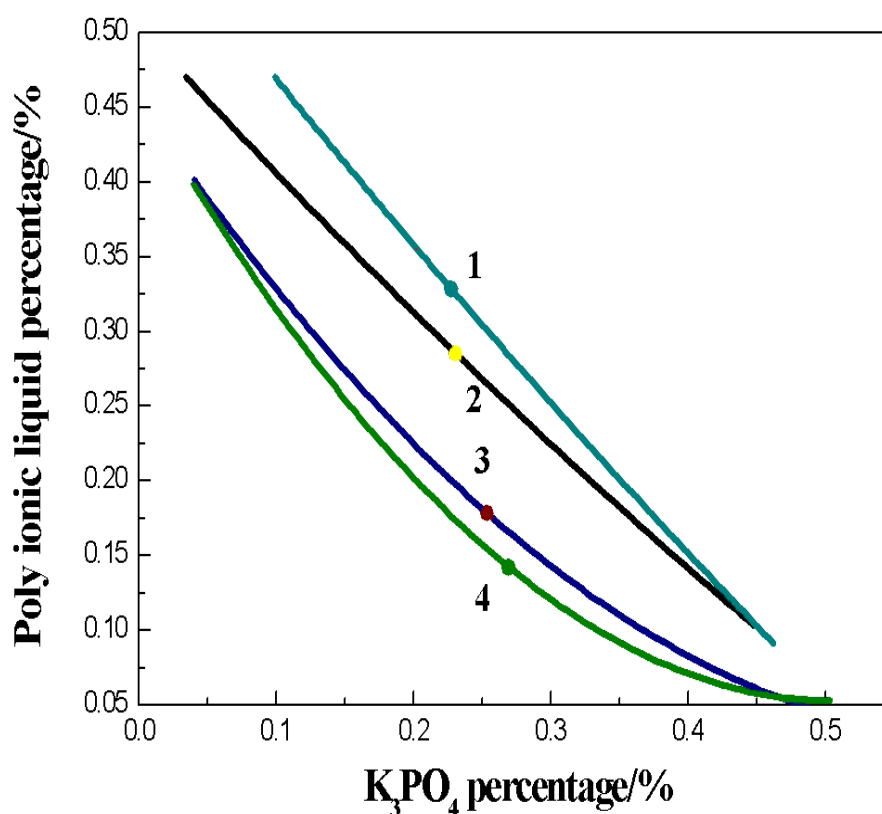
Fig.2: Phase Diagrams of PIL -K_3PO_4 in ATPE. (n= 2(line1), 4(line 2), 6(line 3) and 8(line 4)

2.3.4 Response Surface Optimization Design

PIL and K_3PO_4 aqueous two-phase system extraction rate of metal ions include: the ionic liquid anion and cation species, inorganic salt type, the type and amount of auxiliary complexing agent, pH and temperature, the experimental A three-factor three-level response surface model was established by Box-Behnken method according to the amount of EDTA, pH and temperature. The average of three measurements was fitted by the following second-order linear equation [10]

$$Y = \beta_0 + \sum_{i=1}^{k} \beta_i X_i + \sum_{i=1}^{k} \beta_{ii} X_i + \sum_{i=1}^{k-1} \sum_{j>1}^{k} \beta_{ij} X_i X_j$$

2.4 Procedure for Extraction

A 40.0 mL of the working solution or aqueous sample and 0.05 g of PIL, 0.05 g of K_3PO_4 (pH=7.0) and 0.05 mL of allura red standard or sample solution were added and transferred into a centrifuge tube and subsequently shaken for 15 min at room temperature. Then, the AR was analyzed using UV-2550-vis spectrophotometer at 246 nm.

2.5 Sample Preparation

1.000 g of Candy was weighed in a small beaker after grinding into powder. The powder was dissolved in 30 mL distilled water at 60 ℃ ultrasonically extracted for 30 min and then filtered and was poured into 250.0 mL flask then dissolved with distilled water.

5.000 g beverage(fruit juice) was transferred into a 100.0 mL volumetric flask and dissolved in deionized water. The sample solution was put in the darkness at 4℃.

III. RESULTS AND DISCUSSION

3.1 Characterization of PIL by FTIR

The FTIR spectra of PIL (Fig. 3) was significantly reduced due to the characteristic absorption of imidazole groups, the transmittance at wave numbers 591 and 733 cm^{-1} was due to P-F stretching vibration in the PILs, which showed that PILs were well immobilized on the surface of ATPE systems .
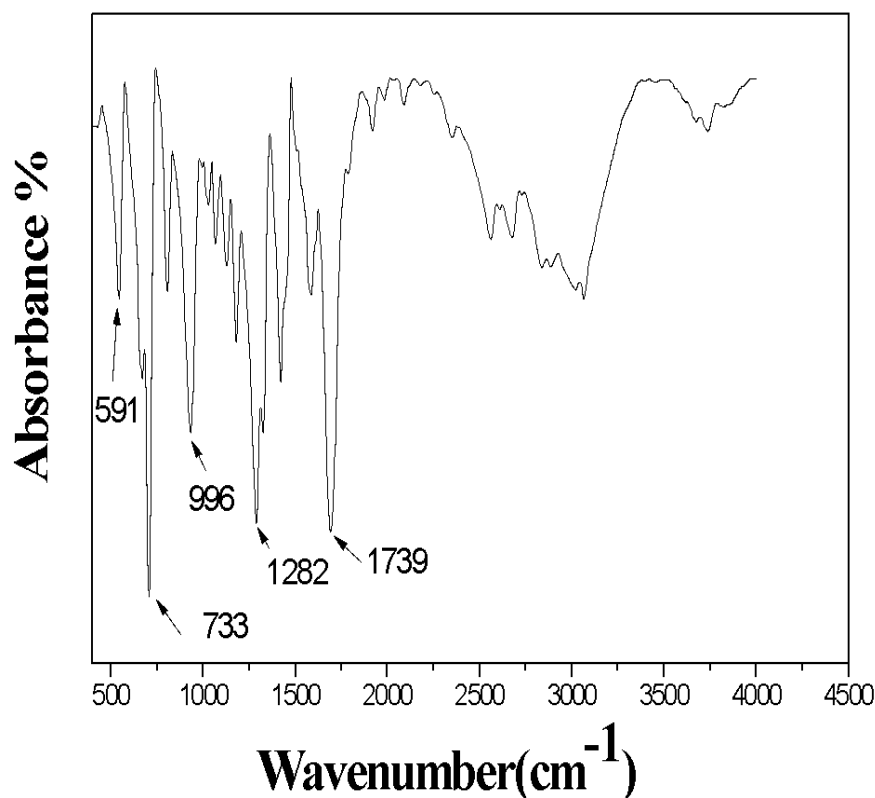
Fig. 3: FT-IR spectra of PIL

3.2 ATPE System Phase Diagram

Double junction of ATPE can provide the minimum concentration of ionic liquid and inorganic salt and the volume ratio of upper and lower phases required to form a dual aqueous phase. The double junction line near the coordinate axis has good phase-forming ability and can produce better Separation effect and

enrichment multiple [11]. According to the reported literature, P_4O_3- has a large free energy of hydration and possesses a good capability of phase formation [12]

3.3 Effect of PH value

PH is one of the important parameters for extraction of AR onto PIL. There were aromatic

Poly Ionic Liquid based Aqueous Two-Phase Extraction Coupled with UV Spectrophotometry for Separation/analysis of Allura Red in Food

12 Volume 23 | Issue 2 | Compilation 1.0 © 2023 Great Britain Journals Press

and azo in the structure of AR, so, its adsorption on PIL occurs mainly by π–π hydrophobic dispersion interaction and weak dipolar force mechanisms. The pH range of the procedure was investigated and optimized between pH 8.0 and 12.0. As shown in (Fig. 4), the extraction efficiency of AR was varied with the pH value. It could be concluded that the extraction efficiency of AR on PIL was increasing to 0.7 when the pH values were 8.0-9.0, then it was approximately constant pH value at 8.0, it is highly possible that AR have been completely ionized(AR⁻) at these pH values and this because of negative charge of the pigment and repulsive force[13], the extraction efficiency decreased to above 0.6 % between the pH value11.0 and 12.0 and this due to the decrease of hydrogen bonding interaction [14].
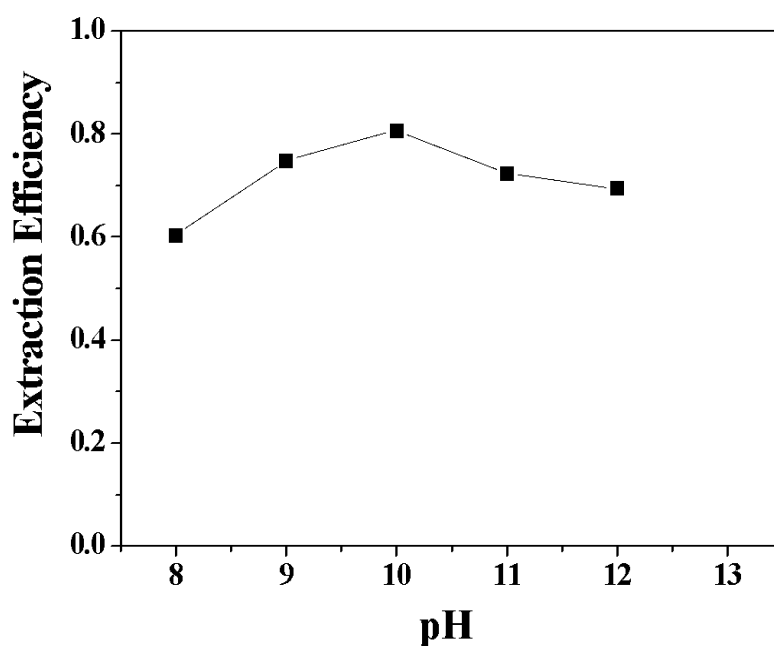
Fig. 4: Effect of pH on Extraction Efficiency

3.4 Effect of K_3PO_4 salt Amount

Fixed Allura red amount of 0.5 mL , PIL from 0.5g K_3PO_4 salt was added 0.5-3.0g Results showed that the extraction rate of PIL on allura red was the highest at 0.5g of K_3PO_4 salt(88%), then it decreased to(80%) , then remained unchanged (Fig.5). So 0.5g of K_3PO_4 salt was used.
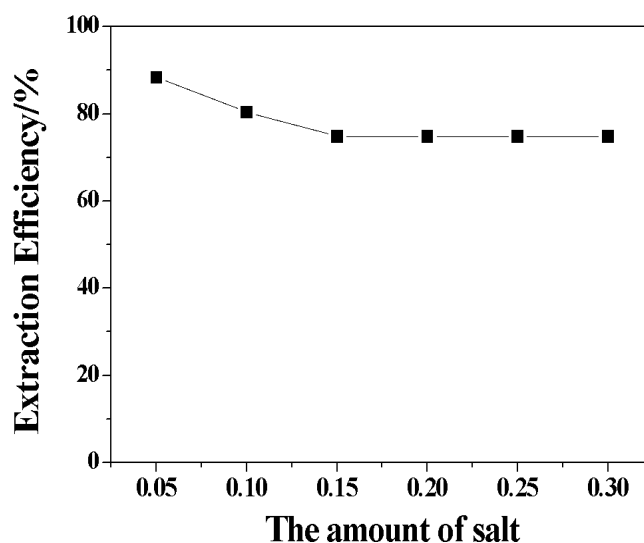
Fig. 5: Effect of Salt Amount on Extraction Efficiency

Poly Ionic Liquid based Aqueous Two-Phase Extraction Coupled with UV Spectrophotometry for Separation/analysis of Allura Red in Food

© 2023 Great Britain Journals Press

Volume 23 | Issue 2| Compilation 1.0

13

London Journal of Engineering Research

3.5 Adsorption Temperature

The extraction efficiency of AR on Fe$_3$O$_4$@SiO$_2$@PIL MNPs at various temperatures (5-60℃) were investigated (Fig.6). The extraction efficiency of AR was increasing from 5℃ to 15℃ and then it decreased and increasing from 20℃ to 60℃. The experiment was done at 25℃.
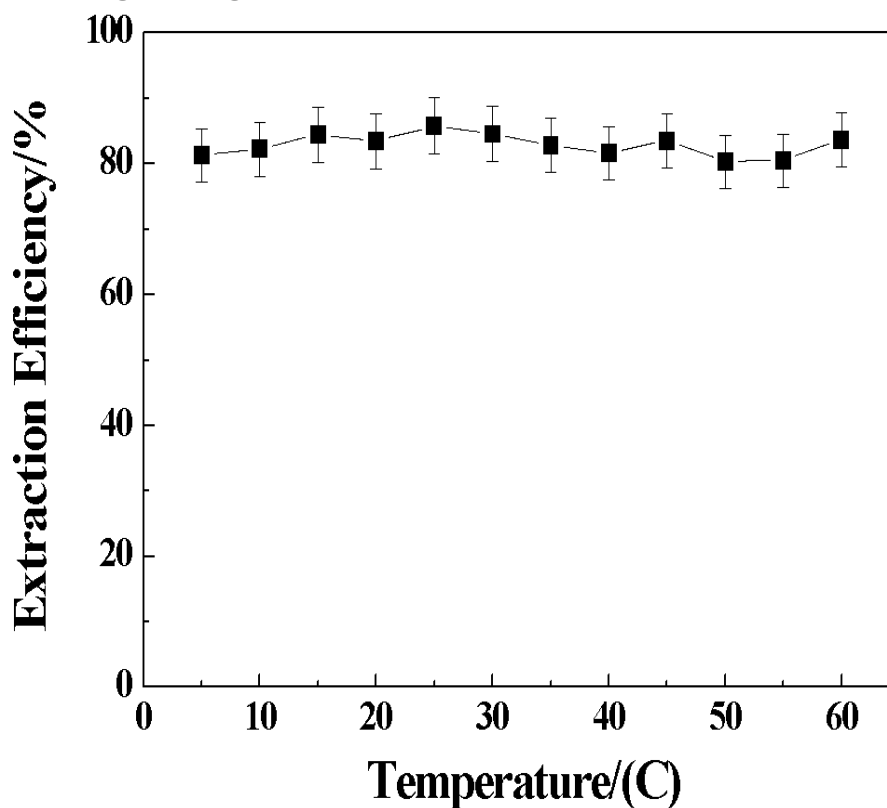
Fig. 6: Effect of Temperature on Extraction Efficiency

3.6 Capacity of Adsorption

The capacity of adsorption is known as the highest volume of allura red adsorbed per gram of PIL MNPs. The adsorption capacity of AR on PIL MNPs was studied (Figure. 7).

When the concentration of AR was 70.0µgmL^{-1}, the adsorption of Allura red reached the maximum. The adsorption capacity for PIL is calculated as 10.45 mg g^{-1}.

Poly Ionic Liquid based Aqueous Two-Phase Extraction Coupled with UV Spectrophotometry for Separation/analysis of Allura Red in Food

14   Volume 23 | Issue 2|Compilation 1.0   © 2023 Great Britain Journals Press
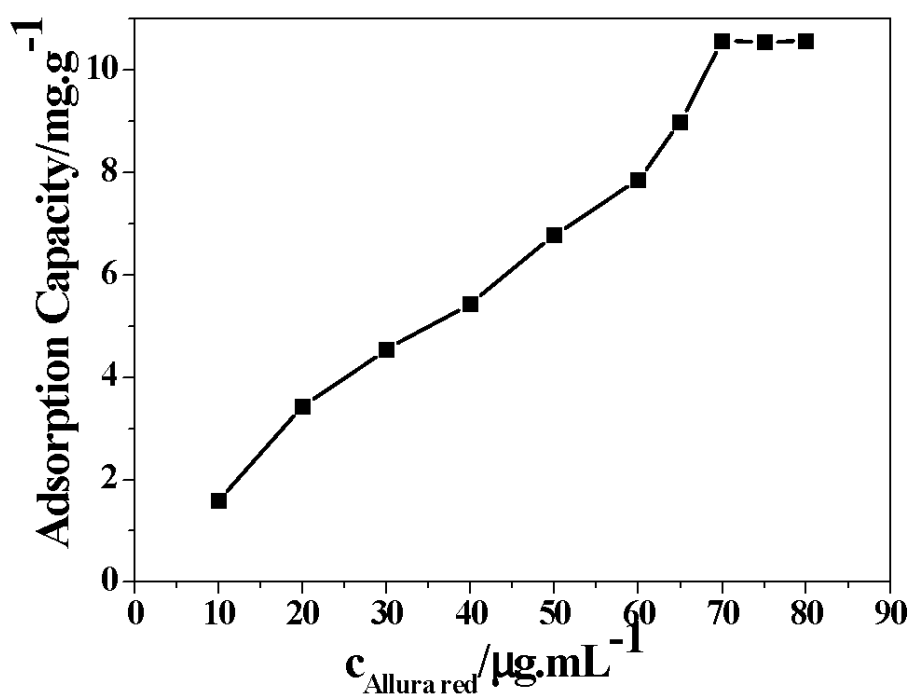
Figure 7: Adsorption capacity

3.7 Interference Effects

The effect of interferents which food samples may contain on separation of Allura red in the availability of interferents was investigated. the tolerance limit for different interferents was as follow, for interferents Zn^{2+}, Ca^{2+}, Mg^{2+}, the tolerance ratio was 102. for interferent Cu^{2+}, tebuconazole ratio was 53, for 2-nitrophenol ratio was 35 and it was 15 for Fe^{3+}, NO_3^-, SO_4^{2-}, Carbendazim, 4-Nitrophenol, phenol. The results showed that most of the foreign substances had no interference with Allura red.

3.8 Analytical Performance

Under optimum conditions described above, the preconcentration factor for AR was 27. The linear range, detection limit (DL), correlation coefficient (R) and relative standard deviation (RSD) were found to be 0.10-9.00 µg/mL, 5.2 µg/L, 0.9987 and 3.10% (n=3, c=4.00 µg/mL).

3.9 Analysis of Sample

This method was introduced to determine the amount of AR in certain brands of some candies and beverages. To further verify for the viability of the method, recovery experiments were carried out, and the AR could be detected in these certain brands of candy and beverage. The obtained values of AR in candies and beverages were measured up to the national standard. To further verify the viability of the method, recovery experiments were carried out (Table 1). The values obtained for unspiked and spiked samples were satisfactory[15].

Poly Ionic Liquid based Aqueous Two-Phase Extraction Coupled with UV Spectrophotometry for Separation/analysis of Allura Red in Food

Table 1: The Recoveries of Allura Red in Candy Samples and Beverages (N=3)

Samples	Added ($\mu g\ mL^{-1}$)	Found ($\mu g\ mL^{-1}$)	Recovery (%)
Candy	0.00	ND	—
	0.50	0.49	98.0
	2.00	2.01	100.5
	4.00	4.13	103.2
Beverages	0.00	0.74	—
	0.50	1.25	102.0
	2.00	2.88	107.0

3.10 Comparison with other Methods

The separation/analysis of AR in real samples was compared with some reported methods, such as solid phase extraction coupled with high performance liquid chromatography, Cloud-point extraction spectrometry, Multi-wall carbon nanotube filmbased electrochemical sensor, solid phase extraction coupled with UV-spectrophotometry and solid phase microextraction coupled with high performance liquid chromatography method were listed in Table 2. Compared with other reported methods, the method adopted in the present work is obviously had good linear range and lower limit of detection and standard deviation using new detector . Moreover, the extraction procedure was simpler and cheaper than that of SPE.

Table 2: Comparison With the Results in Other Literature

Method	Detector	LR ug/ml	LOD $\mu g/L$	RSD (%)	Ref
SPME–HPLC	HPLC	0.05–10.0	9.3	7.8	[15]
Cloud-point extraction spectrometry	UV	0.02-1.40	7.8	3.9	[16]
MWCNT film-based electrochemical sensor	Electrochemical Workstation	0.50-6.00	25.0	NR	[17]
SPE-UV	UV	1.0-6.0	2.4	7.0	[18]
SPE–HPLC	HPLC	0.50-20.0	32.2	6.0	[19]
UV -Spectrophotometry	UV	0.10-9.00	5.2	3.10	This method

NR: Not Reported

3.11 Discussion of Mechanism

The adsorption mechanism could be discussed through extraction isotherms model.

So as to describe extraction capacities for AR by using $Fe_3O_4@SiO_2@PIL$ nanoparticles, the widely used extraction isotherms, Langmuir and Freundlich ones, were introduced. The Langmuir adsorption equations are named as Eq (1).

(1) Langmuir :

$$\frac{C_e}{q_e} = \frac{C_e}{q_{max}} + \frac{1}{q_{max}b} \tag{1}$$

Freundlich model equation is named as Eq. (2):

(2) Freundlich :

$$\ln q_e = \frac{1}{n}\ln C_e + \ln K_F \tag{2}$$

Poly Ionic Liquid based Aqueous Two-Phase Extraction Coupled with UV Spectrophotometry for Separation/analysis of Allura Red in Food

16 | Volume 23 | Issue 2 | Compilation 1.0 | © 2023 Great Britain Journals Press

where q_{max} was the maximum extraction at monolayer coverage (mg g^{-1}), q_e is the AR concentration on the $Fe_3O_4@SiO_2@PIL$ at equilibrium(mgg^{-1}), C_e was the concentration of AR in sample at equilibrium(mgL^{-1}), b is the Langmuir extraction equilibrium constant (Lmg^{-1}), K_F and $1/n$ are the Freundlich characteristic constants, proving the capacity of adsorption and the extraction intensity, respectively. The values of b and q_{max} were calculated by the linear plot of C_e/q_e versus C_e

and the values of K_F and $1/n$ can be obtained from the intercept and slope of the linear plot of $\ln q_e$ versus $\ln C_e$, respectively. The results showed that the linear correlation coefficient for the Langmuir model 0.995 was more than that for the Freundlich one 0.989 (Fig.8). This proved that the Langmuir model fitted the extraction data was better than the Freundlich one. The q_{max} for extraction of AR by the magnetic nanoparticles obtained by the Langmuir isotherm model was 105.80 mgg^{-1}.
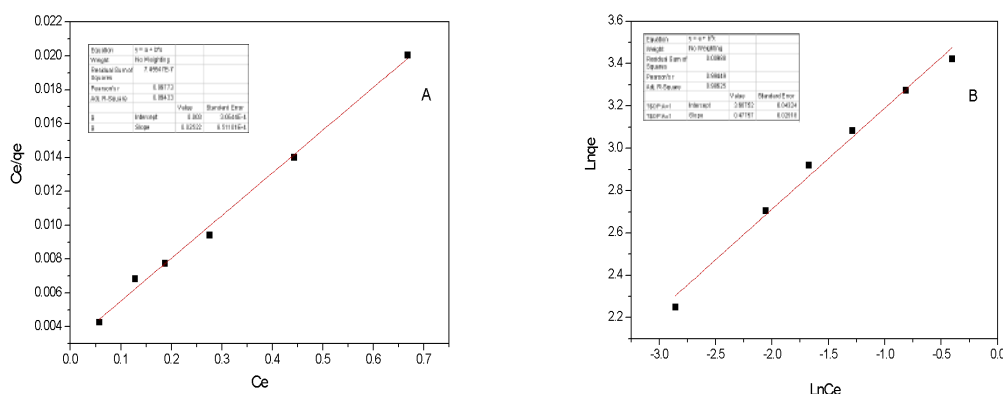
Fig. 8: Adsorption of AR by Langmuir (A) and Freundlich(B) Isotherms Models

IV. CONCLUSION

In this work, PIL was synthesized as aqueous two phase extraction sorbent coupled with UV spectrophotometry to separate/determine AR in food samples. The magnetic separation greatly improved the separation rate and reduced the analysis time. In conclusion, PIL aqueous two phase extraction could be considered as a promising alternatives for the extraction of AR. This introduced method for the separation of allura red from real samples was proved to be satisfactory.

ACKNOWLEDGEMENTS

REFERENCES

1. Shao SW, Nie XM, Wen S, Wang Y, Chen Y, Liu XY (2010) Determination of allura red in salted and pickled vegetables by high performance liquidchromatography. J Chin Health Lab Technol 20: 279-280.

2. Abramsson-Zetterberg L, Ilbäck NG (2013) The synthetic food colouring agentAllura Red AC (E129) is not genotoxic in a flow cytometry-based micronucleusassay in vivo. Food Chem Toxicol 59: 86-89.

3. Bonan S, Fedrizzi G, Menotta S, Elisabetta C (2013) Simultaneous determinationof synthetic dyes in foodstuffs and beverages by high-performance liquidchromatography coupled with diode-array detector. Dyes Pigm 99: 36-40

4. Rao T D, Chen S H, Zhang L Y, Fu C(2012) Determination of allura red in food byspectrometry with magnetic separation and concentration. Chin J Spectrosc Lab29: 2164-2168

5. Chanlon S, Joly-Pottuz L , Chatelut M, Vittori O, Cretier JL (2005) Determination of carmoisine, Allura red and Ponceau 4R in sweets and soft drinks by differential pulse

Poly Ionic Liquid based Aqueous Two-Phase Extraction Coupled with UV Spectrophotometry for Separation/analysis of Allura Red in Food

polarography. J Food Compos Anal 18:503-515

6. A. Eftekhari; O. Seddiki (2017). "Synthesis and Properties of Polymerized Ionic Liquids". European Polymer Journal. 90: 245–272

7. P.A. Rosa, I.F. Ferreira, A.M. Azevedo, M.R. Airesbarros (2010) Aqueous two-phase systems: A viable platform in the manufacturing of biopharmaceuticals,Journal of Chromatography A 1217:2296-2305

8. K.E. Gutowski, G.A. Broker, H.D. Willauer, J.G. Huddleston, R.P. Swatloski, J.D.H. And, R.D. Rogers (2003) Controlling the Aqueous Miscibility of Ionic Liquids: Aqueous Biphasic Systems of Water-Miscible Ionic Liquids and Water-Structuring Salts for Recycle, Metathesis, and Separations, Journal of the American Chemical Society 125:6632.

9. Z. Li, Y. Pei, H. Wang, J. Fan, J. Wang (2010) Ionic liquid-based aqueous two-phase systems and their applications in green separation processes,Trac Trends in Analytical Chemistry 29:1336-1346.

10. S. Chen, Z. Zeng, N. Hu, B. Bai, H. Wang, Y. Suo (2018) Simultaneous optimization of the ultrasound-assisted extraction for phenolic compounds content and antioxidant activity of Lycium ruthenicum Murr. fruit using response surface methodology, Food Chemistry 242:1

11. C. Wu, J. Wang, H. Wang, Y. Pei, Z. Li (2011) Effect of anionic structure on the phase formation and hydrophobicity of amino acid ionic liquids aqueous two-phase systems, Journal of Chromatography A 1218:8587-8593.

12. C. Wu, J. Wang, Z. Li, J. Jing, H. Wang (2013) Relative hydrophobicity between the phases and partition of cytochrome-c in glycine ionic liquids aqueous two-phase systems,Journal of Chromatography A 1305:1

13. Bişgin AT, Uçan M, Narin I (2015) Comparison of Column Solid-Phase Extraction Procedures for Spectrophotometric Determination of E129 (Allura Red) in Foodstuff, Pharmaceutical, and Energy Drink Samples. Journal of AOAC International, 98:(4) 946-952.

14. Bagheri A R, Ghaedi M, Asfaram A, Bazrafshan A A, Jannesar R (2016) Comparative study on ultrasonic assisted adsorption of dyes from single system onto Fe_3O_4 magnetite nanoparticles loaded on activated carbon: experimental design methodology. Ultrasonics Sonochemistry, 34:294–304.

15. Li W J, Zhou X, Tong S S, Jia Q (2013) Poly (N- isopropylacrylamide-co-N, N′-methylene bisacrylamide) monolithic column embedded with γ-alumina nanoparticles microextraction coupled with high-performance liquid chromatography for the determination of synthetic food dyes in soft drink samples. Talanta. 105 :386–392.

16. Yu Y, Fan Z (2016) Magnetic solid-phase extraction coupled with HPLC for the determination of Allura Red in food and beverage samples. Food Additives & Contaminants: Part A, 33:(10) 1527-1534.

17. Pourreza N, Rastegarzadeh S, Larki A (2011)Determination of Allura red in food samples after cloud point extraction using mixed micelles. Food Chem. 126: 1465–1469.

18. Zhang Y, Zhang X J, Lu X H, Yang J Q, Wu K B (2010) Multi-wall carbon nanotube film-based electrochemical sensor for rapid detection of Ponceau 4R and Allura Red. Food Chem. 122: 909–913.

19. Soylak M, Unsal Y E, Tuzen M (2011) Spectrophotometric determination of trace levels of allura red in water samples after separation and preconcentration. Food Chem Toxicol 49(5) :1183–1187.

Poly Ionic Liquid based Aqueous Two-Phase Extraction Coupled with UV Spectrophotometry for Separation/analysis of Allura Red in Food

Electroencephalography in Determining Mood in Animals

Inci Bilge & Emre Aydemir

Mehmet Akif Ersoy University

ABSTRACT

Electroencephalography is one of the most common methods used in the interpretation of neurological activities in the brain of humans and various model animals. With the electroencephalography method, it is possible to obtain information about the various changes that occur in the model creature, its relationship between species, and its emotional state. It is observed that various behaviors are exhibited in model animals due to some factors such as mood, sleep disorder, epilepsy, depression, pain, drug use, addiction, genetics, and environmental.

When these behaviors are examined in the studies; neurodevelopmental disorders, mood disorders, olfactory disorders, visual attention dysfunction, sleep disorders, brain dysfunction, learning disorder, various adjustment, autistic-like behavioral disorders, autism, attention deficit, hyperactivity, anxiety, aging, traumatic brain injury, repetitive grooming It has been observed to cause various behaviors such as social deficits, decreased activity, anxiety, fear conditioning, calmness, staring, anxiety, fear, learning disability, intermodal recognition memory, and depression.

Keywords: model animal, behavior, neuroscience, mood, electroencephalography.

Classification: DDC Code: 616.8 LCC Code: RC346

Language: English

Electroencephalography in Determining Mood in Animals

Inci Bilge[α] & Emre Aydemir[σ]

ABSTRACT

Electroencephalography is one of the most common methods used in the interpretation of neurological activities in the brain of humans and various model animals. With the electroencephalography method, it is possible to obtain information about the various changes that occur in the model creature, its relationship between species, and its emotional state. It is observed that various behaviors are exhibited in model animals due to some factors such as mood, sleep disorder, epilepsy, depression, pain, drug use, addiction, genetics, and environmental.

When these behaviors are examined in the studies; neurodevelopmental disorders, mood disorders, olfactory disorders, visual attention dysfunction, sleep disorders, brain dysfunction, learning disorder, various adjustment, autistic-like behavioral disorders, autism, attention deficit, hyperactivity, anxiety, aging, traumatic brain injury, repetitive grooming It has been observed to cause various behaviors such as social deficits, decreased activity, anxiety, fear conditioning, calmness, staring, anxiety, fear, learning disability, intermodal recognition memory, and depression.

The results of the studies show that these behaviors are closely similar to electroencephalographic humans and various model animals. This study, it is aimed to give information about the state of hearing between humans and various model animals with the method of electroencephalography.

Keywords: model animal, behavior, neuroscience, mood, electroencephalography.

Author α: Department of Electricity and Energy, Vocational School of Technical Sciences, Mehmet Akif Ersoy University, 15100 Burdur, Turkey.

σ: Department of Animal Science, Faculty of Agriculture, Akdeniz University, 07070 Antalya, Turkey.

I. INTRODUCTION

From the moment of their existence, animals exhibit innate and acquired behaviors. Innate behavior; is an instinctive stereotyped movement pattern or reflex-type behavior that occurs due to a stimulus without the need for experience (Aydemir and Bilge 2022). For example, the female animal suckling her young after pregnancy. Apart from this, it is observed that animals exhibit behaviors such as the defense of the area, competition behaviors, and communication in social groups.

It is observed that they exhibit various behaviors for temporary periods that occur under the influence of illness, pain, and medication. But; as a result of factors such as anxiety and stress, they exhibit abnormal behaviors such as phobia (Aydemir and Bilge 2022). Such behaviors are passed down through generations through genes specific to the species.

In many behaviors, it can be acquired later with environmental adaptations (Aydemir and Bilge 2022). Apart from the normal behavior typical of all animals species; aggression behaviors in line with environmental effects such as fear, different light wavelengths, different sound frequencies, heat, stress (status-related attack, intermale attack), predatory attack, idiopathic anger attack (idiopathic rage), fear-based attack (fear-induced), territorial and instinctive attack (maternal), environmentally damaging behaviors, coprophagia, social behavior and agonistic behaviors, urination or defecation outside the designated place, urine marking, wool (cloth) sucking, abnormal behaviors such as aggression are exhibited (Sambraus 1998; Blackshaw 1991;

London Journal of Engineering Research

Aydemir and Bilge 2022). For example; in animals, abnormal behaviors are exhibited due to many physiological changes such as an increase in corticosterone levels, and immune, metabolic, and sleep disorders (Wang et al. 2017; Dolensek et al. 2020).

All these behaviors exhibited are a psychological indicator of the emotional state of the animal (Bilge and Aydemir 2022; Aydemir and Bilge 2022; Aydemir et al. 2021). These psychological indicators are very similar to humans. For example; Behaviors such as depression, social avoidance, anhedonia, passive coping, and learned helplessness observed in humans are similar to the behaviors exhibited in animals (Tye 2018; Muir et al. 2018). Moreover; is observed that many model animals such as mice and monkeys exhibit similar behaviors in many diseases such as depression, chronic stress, sleep disorders, and epileptic seizures observed in humans (Brittlebank et al. 1993; Grandjean et al. 2016; Gadad et al. 2013) and Crawley 2012; According to Jaramillo et al. 2016; Dhamne et al. 2017; Citraro et al. 2019; Roebuk et al. 2020; According to Cai et al. 2020; According to Gandal et al. 2010; Dringenberg 2000). This gives information about the behavior between humans and animals. Various behavioral tests, biomarkers, and Electroencephalograms are used to measure this information (Roach et al. Mathalon, 2008; Koenig et al., 2005).

Electroencephalograms (EEG) are a non-invasive technique that allows the measurement of electrical brain activity in a human or model animal. It can also record brain signals thanks to its high temporal resolution (Ward 2003; Lopes and MEG 2013). These recorded signals are a good source for obtaining information about the neurological status of the model creature (Saminu et al., 2021).

II. ELECTROENCEPHALOGRAPHY (EEG) IN MODEL ANIMALS

Electroencephalography in model animals is a method used to functionally examine the electrical signals produced as a result of neurological activities in the brain (Ward 2013-2015; Bear et al. 2016; Lopes and MEG 2013). Thanks to this method, information is obtained about normal and abnormal functioning in the brain.

Electroencephalography reflects the total slow dendritic potentials of many cortical pyramidal neurons. EEG rhythms in different frequency bands arise from dynamic interactions between populations of neurons and are associated with several different cognitive processes. With this association, EEG recordings show abnormalities in brain functioning (Ward 2013-2015; Bear et al. 2016; Lopes and MEG 2013).

It has also been used in the diagnostic criteria of various psychiatric disorders such as schizophrenia, bipolar disorder, sleep disorder, attention-deficit/hyperactivity disorder (ADHD), and Alzheimer's disease, especially in recent years (Roach et al. Mathalon, 2008; Yordanova et al., 2001; Koenig et al., 2005). It is known that the Prefrontal, Orbitofrontal, and Insular Cortices mPFC and its inputs/outputs are involved in behaviors related to anxiety and mood in psychological and psychiatric diseases such as these (Kheirbek et al. 2012; Kheirbek and Hen 2014). Polysomnography, which is used in the diagnosis of sleep disorder, provides information about brain electrical activity (EEG), sleep stages, sleep quality, muscle activity (EMG), respiratory rate, eye movements (EOG), heart rhythm (ECG) and physiological states of activities in sleep stages (Boulos). et al. 2019; Weber and Dan, 2016; O'Donnell et al. 2018). Recording the electrical activity of the brain with electrodes placed on the scalp is called Electroencephalography (EEG).

They observed that repetitive grooming, social deficits, decreased activity, anxiety, learning problems, reduced fear conditioning, olfactory disorders, hyperactivity, and various autistic-like behavioral disorders occur in the model animal (Jaramillo et al. 2016; Dhamne et al. 2017; Balzamo). et al. 1998; Gadad et al. 2013; Crawley 2012; Cao et al. 2020; Radyushkin et al. 2009; Liu et al. 2017).

Thanks to the electroencephalography obtained from these behavioral disorders, it is possible to comment on the relations between the species.

London Journal of Engineering Research

III. DISCUSSION

When many studies on animals and humans are examined; is observed that there is a close relationship between the emotional states of animals and humans. As an indicator of this close relationship; is stated that facial expressions in mice reflect internal emotional states, just like facial expressions in humans (Dolensek et al. 2020; Stringer et al. 2019).

There are many examples like this. Electroencephalography of these samples is functionally obtained by electroencephalography of the electrical signals produced as a result of neurological activities in the brain (Ward 2013-2015; Bear et al. 2016; Lopes and MEG 2013; Gandal et al. 2010; Dringenberg 2000).

In the results of many studies, they reported that neuronal activities were similar between human and animal experiments according to electroencephalography recordings (Videman et al. 2016; Fedor et al., 2010; Colas et al., 2005; de Vries et al., 2005).

For example; It is stated that close similarities are observed in the electroencephalography of pathological conditions such as neurode-velopmental disorders, autism, attention deficit hyperactivity, mood disorder, anxiety, and adjustment disorders, brain dysfunction, learning disability, aging, and traumatic brain injury (Fedor et al., 2010; Colas et al., 2005). ; de Vries et al., 2005).

3.1 Mood

Brittlebank et al. (1993) in the results of a study; In the case of depression, people are prejudiced against overgeneralization; reported that animals exhibit simple behaviors such as avoidance and approach as an indicator of their internal emotional state. In the results of another study, Grandjean et al. (2016) determined that increased amygdala-PFC functional connectivity and white matter structural changes in the cingulum showed similarity in mice and humans against chronic stress. The results of a study by Xunxun Chu (2019) reported that the naturally induced

depression models in macaques are very similar to the human depression model.

3.2 Sleeping Disorder

When examining studies on sleep disorders, Gadad et al. (2013) and Crawley (2012) reported in the results of the study that there is a similarity between the symptoms of sleep disorders between animal models and humans. According to Jaramillo et al. (2016) and Dhamne et al. (2017) as a result of sleep disturbance in Shank3 knockout mice; they observed the emergence of repetitive grooming, social deficits, decreased activity, anxiety, learning problems, and various autistic-like behavioral disorders.

In another similar study, Cao et al. (2020) reported that abnormal behaviors and seizures due to sleep disturbance were observed in Neuroligin-2 knockout mice. Radyushkin et al. (2009) and Liu et al. (2017), it was observed that Neuroligin-3 knockout mice preferred reduced fear conditioning, olfactory disorders, and hyperactivity, as well as reduced ultrasound vocalization and social innovation due to sleep disturbance. On the other hand, Monassi et al.

(2003), Andersen and Tufik (2003), in the results of the studies against a living thing that affects from the outside; observed that they exhibit temporary or permanent changes in behavior.

Moreover; they also found that their mice showed sleep disorders. Armitage (2007) found in a study that electroencephalography findings were more than 80% of patients with depression and that these people had sleep disorders.

3.3 Epilepsy

Citraro et al. (2019) examined the development of epileptic seizures and behavioral changes in mice with EEG. In the results obtained by the study results; They reported that it could represent a promising new therapy to prevent and treat the epileptogenic process and associated behavioral and cognitive changes. In another similar study, Roebuk et al. (2020) reported that the results of genetic absence epilepsy EEGs in mice include behavioral stagnation, staring, anxiety, fear,

Electroencephalography in Determining Mood in Animals

learning disability, and dysfunction in intermodal recognition memory and visual attention.

Electroencephalography is an important tool for characterizing epilepsy in tuberous sclerosis complex mouse models (Magri et al., 2011; Zeng et al., 2008). Background EEG spectral analysis is commonly used to investigate.

3.4   Some Environmental Factors

In addition to all these, when studies conducted in line with environmental effects such as fear, different wavelengths of light, different sound frequencies, temperature, and stress are examined, Gavales et al. (1970) studied the effects of low-level, low-frequency electric fields on monkeys' behavior and EEGs. In the results of the study, monkeys under 7 c/s fields reported significantly faster reciprocal response time in 5 of the 6 experiments. In addition, the results of the analysis of the EEG data showed that the average differences between open and closed areas were more than 0.4 seconds; reported that all monkeys showed a relative power peak in the frequency of the areas (10 c/sec and 7 c/sec) for the hippocampus. In some studies, Stephenson et al.

(2012), Glickman et al. (2006), Strong et al. (2009), Cajochen et al. (2000), and Beersman (2003), on the other hand, examined the relationship between daylight and behavior. In the results of the study, they reported that electroencephalography data affected mood, depression, behavior, sleep disorders, and physiological and chemical functions.

In another study, Hallaschmid et al. (2002) examined whether reward in humans is associated with EEG synchronization similar to that seen in animals. In the results of the study, the researchers reported that increased beta activity during drinking and sucking in thirsty subjects likely reflects nonspecific activation related to the motivational power of sensorimotor regulation during consumption behavior.

They also stated that low alpha synchronization due to thirst after drinking, which is created not only by water consumption but also by surrogate oral stimuli, is a reflection of the impulse-reducing and rewarding qualities of oral stimulus and consumption behavior.

3.5   Genetic

Among the factors affecting behavior in model animals; genetic factors, age, gender, physiological, and hormonal conditions are included. In the results of a study using mice as model animals, Cambiaghi et al. (2012) reported that tuberous sclerosis complex caused by benign tumors in different organs and serious neuropsychiatric symptoms such as epilepsy, intellectual disability, autism, anxiety, and depressive behavior can be determined by EEG method. Also, Cambiaghi et al. (2012) found that anxiety and depression were reduced in mutant mice treated with rapamycin in their EEG power spectrum results.

Carter (1978) reported that it produced a trance-like stupor in all monkeys associated with marked EEG changes and hypothermia in adult and preadolescent rhesus monkeys. Researchers have also found that characteristic EEG and behavioral changes are age-related. In another study, Cai et al. (2020) examined expression networks, locomotive, and cognitive behaviors, and EEG and gene-circuit-behavior analyses in genetically modified monkeys. The results of the study; reported that decreased β-synchronization in front-parietal-occipital networks was associated with abnormal locomotive behaviors.

Blackburn-Munro (2004), who conducted a study on genetically manipulated animals, stated that there are many pathological changes similar to various chronic pain in humans in animal models of chronic pain, using it together with classical physiological and biochemical measurements according to EEG results. Moreover; reported that the evaluation of pain and stress with the EEG method in animals is an alternative method.

Tuberous sclerosis Complex is a multisystem genetic disorder caused by mutations in the Tsc1 or Tsc2 genes that lead to hyperactivation of the m TOR pathway, a key signaling pathway for synaptic plasticity.

3.6 Pain

Joyce and David (2019), who conducted a study on rats, mice, and monkeys, examined the electroencephalography of acute and chronic pain.

In the results of the study, the researchers observed that the transition from acute pain to chronic pain resulted in significant changes in brain function.

Moreover; they reported that brain activations in acute pain are related to the sensory aspect of noxious stimuli, including the primary somatosensory cortex, insula, cingulate cortex, thalamus, retrosplenial cortex, and periaqueductal gray.

Ong et al. (1997) measured acute pain in sheep and examined changes in both the electroencephalogram frequency spectrum and behavioral responses to increased electrical stimulation in sheep.

In the results of the study, they stated that the human acute pain model can be applied to sheep and that these electroencephalogram changes can provide a good measure for acute pain in sheep.

37. Medicine

Van Lier et al. (2004), Graversen et al. (2012) Leocani et al. (2000), and Barry et al. (2009); In the studies conducted by Cambiaghi et al. (2012) Baumann et al. (2006) stated that the changes in the brain caused by the drug efficacy in humans and animal models are closely related to behavior.

They reported that these relationships are a frugal indicator between EEG data and behavior. They found a slight but significant reduction in theta and alpha mean dominant frequency (MDF) with behavioral changes in rapamycin-treated wild-type mice, suggesting a mild brain dysfunction associated with the drug treatment studies by Salinsky et al. (2004), Leocani et al., (2000, 2010), Klimesch (1999), and Klimesch, (1997). They reported that this resulted in a mild brain dysfunction associated with drug therapy.

They also observed that EEG slowing in humans is associated with neurological disorders or even lower working memory, IQ or drug-induced lethargy, and cognitive impairment in healthy subjects.

3.8 Dependence

Howard (2000) examined the electroence-phalography of the brain functioning in various animal models with alcohol dependence. The researcher reported that there are physiological and behavioral advantages and disadvantages to alcohol withdrawal syndrome. The researcher also stated that it may affect enhanced autonomic nervous system activation, sensory hyperreactivity, convulsions, anxiety, and dysphoria.

When other similar studies are examined, Walker and Zornetzer (1974), Ehlers and Chaplin (1991), Poldrugo and Snead (1984), and Perrin et al. (1975) reported that EEG abnormalities were associated with alcohol withdrawal in various model animals, including mice, rats, cats, and primates.

IV. CONCLUSIONS

There are various behaviors that they exhibit depending on the various moods observed in humans and various model animals. These behaviors vary depending on some factors such as mood, sleep disorder, epilepsy, depression, pain, drug use, addiction, genetics, and environmental.

Neurodevelopmental disorders, mood disorders, olfactory disorders, visual attention dysfunction, sleep disorders, brain dysfunction, learning disorders, various adjustment, and autistic-like behavior disorders, autism, attention deficit, hyperactivity, anxiety, aging, traumatic brain injury in various model animals. It has been observed that various behaviors such as repetitive grooming, social deficits, decreased activity, anxiety, fear conditioning, calmness, staring, anxiety, fear, learning disability, intermodal recognition memory and depression are exhibited.

It has been observed that these behaviors closely resemble each other among various species of electroencephalography.

REFERENCES

1. Andersen, M.L. and Tufik, S., 2003. Sleep patterns over 21-day period in rats with chronic constriction of sciatic nerve. Brain Res., 984, 84 – 92 .

2. Armitage, R., 2007. Sleep and circadian rhythms in mood disorders. Acta Psychiatrica Scandinavica., 115(s433), 104–115.

3. Aydemir E. And Bilge İ., 2022. Animal Psychology- BEHAVİOR AND TEMPERAMENT IN CATS AND DOGS. LAP LAMBERT Academic Publishing – ISBN., 978-620-4-75264-8.

4. Barrett, L.F.; Adolphs, R.; Marsella, S.; Martinez, A.M.; Pollak, S.D., 2019. Emotional expressions reconsidered: Challenges to inferring emotion from human facial movements. Psychol. Sci. Public Interest., 20, 1–68.

5. Barry, R. J., Clarke, A. R., Hajos, M., Mc Carthy, R., Selikowitz, M., Bruggemann, J. M., 2009 Dec. Acute atomoxetine effects on the EEG of children with attention- deficit/ hyperactivity disorder. Neuro- pharmacology., 57 (7e8), 702e707.

6. Baumann, C. R., Kilic, E., Petit, B., Werth, E., Hermann, D. M., Tafti, M., Bassetti, C. L., 2006. Sleep EEG changes after middle cerebral artery infarcts in mice: different effects of striatal and cortical lesions. Sleep., 29, 1339e1344.

7. Balzamo, E., P. Van Beers, D. Lagarde., 1998. Scoring of sleep and wakefulness by behavioral analysis from video recordings in rhesus monkeys:comparison with con- ventional EEG analysis, Electroencephalogr. Clin. Neurophysiol., 106 (3); 206–212.

8. Bear, M. F., Connors, B. W., and Paradiso, M. A., 2016. "Neuroscience: Exploring the Brain", Neuroscience: Exploring the Brain: Fourth Edition, 4th ed. Ed., Wolters Kluwer, Philadelphia., 13–21, 180–190, 223, 646–658.

9. Beersma DG., 2003. Model sofhuman sleepregulation. In:Billiar dM, editor. Sleep: physiology, investigations and medicine. New York: Kluwer Academic/Plenum Publishers., 61e70.

10. Bilge İ. and Aydemir E., 2021. Interpretation Of The Relationship Between The Effects Of Different Colors Wavelength Light Application And Sound Frequency In Japanese Quails By Spectral Analysis. Techno-Science, vol. 4. 2. 40-49.

11. Bilge İ. and Aydemir E. 2022. Tıme-Frequency Analysıs And Examınatıon Of Responses To Dıfferent Color Waves Dependıng On Sex In Japanese Quaıls (Behavıor And Adaptatıon Wıth Anımal Sound) Lap Lambert Academic Publishing.

12. Bilge İ. and Aydemir E., 2022. COMPORTEMENT ET ADAPTATION AVEC LE SON ANIMAL-CAILLES JAPONAISES. Editions Notre Savoir (2022-04-27)- ISBN-13: 978-620-4-60240-0.

13. Blackburn-Munro, G., 2004. Pain-like behaviours in animals – how human are they? Trends in Pharmacological Sciences, 25(6), 299–305.

14. Blackshaw JK., 1991. An overview of types of agressive behaviour in dogs and methods of treatments. Appl. Anim. Behav. Sci., 30, 351-361.

15. Boulos, M. I., Jairam, T., Kendzerska, T., Im, J., Mekhael, A., and Murray, B. J., 2019. Normal polysomnography parameters in healthy adults: a systematic review and meta-analysis. Lancet Respir. Med. 7, 533−543.

16. Brittlebank, A. D., 1993. Autobiographical memory in de- pression: state or trait marker? Br. J. Psychiatry., 162, 118–121.

17. Cai, D.-C., Wang, Z., Bo, T., Yan, S., Liu, Y., Liu, Z., Wang, Z., 2020. MECP2 Duplication Causes Aberrant GABA Pathways, Circuits and Behaviors in Transgenic Monkeys: Neural Mappings to Patients with Autism. The Journal of Neuroscience., 40(19), 3799−3814.

18. Cajochen C, Brunner DP, Krauchi K, Graw P, Wirz-Justice A., 2000. EEG and subjective sleepiness during extended wakefulness in seasonal affective disorder: circadian and homeostatic influences. Biol Psychiatry., 1;47(7):610e7.

19. Cambiaghi, M., Cursi, M., Magri, L., Castoldi, V., Comi, G., Minicucci, F., Leocani, L., 2013. Behavioural and EEG effects of chronic rapamycin treatment in a mouse model of

Tuberous Sclerosis Complex. Neurophar-macology., 67, 1–7.

20. Cannas, S.; Palestrini, C.; Canali, E.; Cozzi, B.; Ferri, N.; Heinzl, E.; Minero, M.; Chincarini, M.; Vignola, G.; Costa, E. D. 2018. Thermography as a Non-Invasive Measure of Stress and Fear of Humans in Sheep. Animals., 8, 146.

21. Cao, F., Liu, J. J., Zhou, S., Cortez, M. A., Snead, O. C., Han, J., 2020. Neuroligin 2 regulates absence seizures and behavioral arrests through GABAergic transmission within the thalamocortical circuitry. Nat. Commun., 11:3744.

22. Citraro, R., Iannone, M., Leo, A., De Caro, C., Nesci, V., Tallarico, M., Russo, E., 2019. Evaluation of the effects of liraglutide on the development of epilepsy and behavioural alterations in two animal models of epileptogenesis. Brain Research Bulletin., 153, 133–142.doi:10.1016/j.brainresbull.2019.08.0 01

23. Colas, D., Cespuglio, R., Sarda, N., 2005 Feb. Sleep wake profile and EEG spectral power in young or old senescence accelerated mice. Neurobiol. Aging 26 (2), 265e273.

24. Crawley, J. N., 2012. Translational animal models of autism and neurodevelopmental disorders. Dialog. Clin. Neurosci., 14, 293–305.

25. de Vries, P., Humphrey, A., McCartney, D., Prather, P., Bolton, P., Hunt, A., 2005. Consensus clinical guidelines for the assessment of cognitive and behavioural problems in tuberous sclerosis. Eur. Child. Adolesc. Psychiatry., 14, 183e190.

26. Dhamne, S. C., Silverman, J. L., Super, C. E., Lammers, S. H. T., Hameed, M. Q., Modi, M. E., et al. (2017). Replicable in vivo physiological and behavioral phenotypes of the Shank3B null mutant mouse model of autism. Mol. Autism 8:26.

27. Dolensek, N., 2020. Facial expressions of emotion states and their neuronal correlates in mice. Science., 368, 89–94.

28. Dringenberg, H.C., 2000. Alzheimer's disease: more than a 'cholinergic disorder'—evidence that cholinergic–monoaminergic interactions contribute to EEG slowing and dementia. Behav. Brain Res., 115 (2), 235–249.

29. Ehlers CR, Chaplin RI., 1991. EEG and ERP response to chronic ethanol exposure in rats. Psychopharmacology., 104:67–74.

30. Fedor, M., Berman, R.F., Muizelaar, J.P., Lyeth, B.G., 2010. Hippocampal dysfunction after lateral fluid percussion injury. J. Neurotrauma., 27, 1605e1615.

31. Gadad, B. S., Hewitson, L., Young, K. A., and German, D. C., 2013. Neuropathology and animal models of autism: genetic and environmental factors. Autism Res. Treat., 2013:731935.

32. Gandal, M.J., Edgar, J.C., Ehrlichman, R.S., Mehta, M., Roberts, T.P., Siegel, S.J., 2010. Validating γ oscillations and delayed auditory responses as translational biomarkers of autism. Biol. Psychiatr., 68 (12), 1100–1106.

33. García-Gutiérrez, M.S., 2020. Biomarkers in psychiatry: concept, definition, types and relevance to the clinical reality. Front. Psychiatry., 11, 432.

34. Gavalas, R. J., Walter, D. O., Hamer, J., & Rossadey, W., 1970. Effect of low-level, low-frequency electric fields on EEG and behavior in Macaca nemestrina. Brain Research., 18(3), 491–501.doi:10.1016/0006-8993(70)90132-0.

35. Glickman G, Byrne B, Pineda C, Hauck WW, Brainard GC. 2006. Light therapy for seasonal affective disorder with blue narrow-band light-emitting diodes (LEDs). Biol Psychiatry., 15;59(6):502e7.

36. Grandjean, J., 2016. Chronic psychosocial stress in mice leads to changes in brain functional connectivity and metabolite levels comparable to human depression. Neuroimage., 142, 544–552.

37. Graversen, C., Olesen, S.S., Olesen, A.E., Steimle, K., Farina, D., Wilder-Smith, O.H., Bouwense, S.A., van Goor, H., Drewes, A.M., 2012. The analgesic effect of pregabalin in patients with chronic pain is reflected by changes in pharmaco- EEG spectral indices. Br. J. Clin. Pharmacol., 73 (3), 363e372.

38. Hallaschmid M., Mölle M., Fischer S., Born J., 2002. EEG synchronization upon reward in man, Clinical Neurophysiology., 113, 7.

Electroencephalography in Determining Mood in Animals

39. Howard C. B., 2000. Animal Models Of Alcohol Withdrawal, Alcohol Research & Health., 24, 2 105-113.

40. Jaramillo, T. C., Speed, H. E., Xuan, Z., Reimers, J. M., Liu, S., and Powell, C. M., 2016. Altered striatal synaptic function and abnormal behaviour in Shank3 Exon4-9 deletion mouse model of autism. Autism Res., 9, 350–375. doi: 10.1002/aur.1529.

41. Joyce T. Da Silva and David Seminowicz, 2019, Neuroimaging of pain in animal models: a review of recent literatüre, Pain Reports, 4(4): e732.

42. Kheirbek, M.A. and Hen, R., 2014. New neurons in the brain keep anxiety at bay. Sci. Am. Published online July www.scientificamerican.com/article/new-neurons-in-the-brain- keep-anxiety-at-bay/

43. Kheirbek, M.A., 2012. Neurogenesis and generalization: a new approach to stratify and treat anxiety disorders. Nat. Neurosci. 15, 1613–1620.

44. Kim, J., Gulati, T., and Ganguly, K., 2019. Competing roles of slow oscillations and delta waves in memory consolidation versus forgetting., 179, 514.e3–526.e3.

45. Klimesch, W., 1997. EEG-alpha rhythms and memory processes. Int. J. Psychophy- siol., 26, 319e340 (IQ).

46. Klimesch, W., 1999. EEG alpha and theta oscillations reflect cognitive and memory performance: a review and analysis. Brain Res. Cogn. Brain Res. Rev., 29 (2e3), 169e195.

47. Koenig, T., Prichep, L., Dierks, T., Hubl, D., Wahlund, L. O., John, E. R., Jelic, V., 2005. Decreased EEG synchronization in Alzheimer's disease and cognitive impairment. Neurobiol., Aging 26 (2), 165–171.

48. Lambert, H.; Carder, G. 2019., Positive and negative emotions in dairy cows: Can ear postures be used as a measure? Behav. Process. 158, 172–180.

49. LeBlanc BW, Bowary PM, Chao YC, Lii TR, Saab CY., 2016. Electroencephalographic signatures of pain and analgesia in rats., 157:2330–40.

50. Leocani, L., Gonzalez-Rosa, J. J., Comi, G., Nov., 2010. Neurophysiological correlates of cognitive disturbances in multiple sclerosis. Neurol. Sci., 31 (Suppl. 2), S249eS253.

51. Leocani, L., Locatelli, T., Martinelli, V., Rovaris, M., Falautano, M., Filippi, M., Magnani, G., Comi, G., 2000. Aug. Electroencephalographic coherence analysis in multiple sclerosis: correlation with clinical, neuropsychological, and MRI find- ings. J. Neurol. Neurosurg. Psychiatr., 69 (2), 192e198.

52. Liu, J. J., Grace, K. P., Horner, R. L., Cortez, M. A., Shao, Y., and Jia, Z., 2017. Neuroligin 3 R451C mutation alters electroen-cephalography spectral activity in an animal model of autism spectrum disorders. Mol. Brain., 10, 10–10.

53. Lopes da Silva, F., 2013. EEG and MEG: Relevance to Neuroscience. Neuron., 80, 1112–1128.

54. Magri, L., Cambiaghi, M., Cominelli, M., Alfaro-Cervello, C., Cursi, M., Pala, M., Bulfone, A., Garcia-Verdugo, J.M., Leocani, L., Minicucci, F., 2011. Sustained activation of mTOR pathway in embryonic neural stem cells leads to develop- ment of tuberous sclerosis complex-associated lesions. Cell Stem Cell., 9, 447e462.

55. Mogil, J. S.; Pang, D. S.; Dutra, G. G. S.; Chambers, C.T. 2020. The development and use of facial grimace scales for pain measurement in animals. Neurosci. Biobehav. Rev., 116, 480–493.

56. Monassi, C. R., 2003. A subpopulation of rats show social and sleep-waking changes typical of chronic neuropathic pain following

57. Peripheral nerve injury. Eur. J. Neurosci., 17, 1907–1920.

58. Morton DL, Sandhu JS, Jones AK., 2016. Brain imaging of pain: state of the art. J Pain Res., 9:613–24.

59. Muir, J., 2019. Wiring the depressed brain: optogenetic and chemogenetic circuit interrogation in animal models of depression. Neuropsychopharmacology 44, 1013.

60. Nasca, C., 2019. Multidimensional predictors of suscep-tibility and resilience to social defeat stress. Biol. Psychiatry 86, 483–491.

61. O. Carter Snead Gamma Hydroxybutyrate İn The Monkey, I., 1978. Electroen-

London Journal of Engineering Research

cephalographic, Behavioral, And Pharmacokinetic Studies Neurology, First Published July 1.

62. O'Donnell, S., Beaven, C. M., and Driller, M. W., 2018. From pillow to podium: a review on understanding sleep for elite athletes. Nat. Sci. Sleep 10, 243–253. doi: 10.2147/nss. s158598

63. Ong, R., Morris, J., O'dwyer, J., Barnett, J., Hemsworth, P., and Clarke, I., 1997. Behavioural and EEG changes in sheep in response to painful acute electrical stimuli. Australian Veterinary Journal, 75(3), 189–193.doi:10.1111/j. 1751-0813.1997.tb10064.

64. Pereira, C.B.; Dohmeier, H.; Kunczik, J.; Hochhausen, N.; Tolba, R.; Czaplik, M. 2019. Contactless monitoring of heart and respiratory rate in anesthetized pigs using infrared thermography. PLoS ONE., 14, e0224747.

65. Perrin RG, Kalant H, Livingston KE., 1975. Electroencephalographic signs of ethanol tolerance and physical dependence in the cat. Electroencephalography and Clinical Neurology., 39:157–162.

66. Poldrugo F, Snead OC. 1984. Electroencephalographic and behavioral correlates in rats during repeated ethanol withdrawal syndromes. Psychopharmacology., 83:140–146.

67. Radyushkin, K., Hammerschmidt, K., Boretius, S., Varoqueaux, F., El-Kordi, A., Ronnenberg, A., 2009. Neuroligin-3-deficient mice: model of a monogenic heritable form of autism with an olfactory deficit. Genes Brain Behav., 8, 416–425. doi: 10.1111/j.1601-183x.2009.00487.

68. Roach, B.J., Mathalon, D.H., 2008. Event-related EEG time-frequency analysis: an overview of measures and an analysis of early gamma band phase locking in schizophrenia. Schizophr. Bull. 34 (5), 907–926.

69. Roebuck AJ, An L, Marks WN, Sun N, Snutch TP, Howland JG., 2020. Cognitive Impairments in Touchscreen-based Visual Discrimination and Reversal Learning in Genetic Absence Epilepsy Rats from Strasbourg. Neuroscience., 430:105-112.

70. Salinsky, M., Spencer, D., Oken, B., Storzbach, D., 2004. Effects of oxcarbazepine and phenytoin on the EEG and cognition in healthy volunteers. Epilepsy Behav., 5, 894e902.

71. Sambraus, H.H., 2002. Aufgaben der Angewandten Ethologie bei Landwirtschaftlichen Nutztieren fr herund heute. Gumpensteiner Tagung "Nutztierhaltung im Wandel der Zeit", Bundesanstalt fralpenl ndische Landwirtschaft, Gumpenstein., A-8952 Irdning: 17-20.

72. Saminu, S., Xu, G., Shuai, Z., Abd El Kader, I., Jabire, A. H., Ahmed, Y. K., Karaye, I. A., Ahmad, I.S., 2021. A Recent Investigation on Detection and Classification of Epileptic Seizure Techniques Using EEG Signal. Brain Sciences., 11, 668.

73. Sawangjit, A., Oyanedel, C. N., Niethard, N., Salazar, C., Born, J., and Inostroza, M., 2018. The hippocampus is crucial for forming non-hippocampal long-term memory during sleep. Nature., 564, 109–113. doi: 10.1038/s41586-018-0716-8.

74. Stephenson, K. M., Schroder, C. M., Bertschy, G. and Bourgin, P., 2012. Complex interaction of circadian and non-circadian effects of light on mood: Shedding new light on an old story. Sleep Medicine Reviews., 16(5), 445–454. doi:10.1016/j.smrv.2011.09.002.

75. Stringer, C., 2019. Spontaneous behaviors drive multidi- mensional, brainwide activity. Science., 364, 255

76. Strong RE, Marchant BK, Reimherr FW, Williams E, Soni P, Mestas R., 2009. Narrow-band blue-light treatment of seasonal affective disorder in adults and the influence of additional nonseasonal symptoms. Depress Anxiety., 26(3):273e8.

77. Tye, K.M. 2018. Neural circuit motifs in valence processing. Neuron 100, 436–452

78. van Lier, H., Drinkenburg, W.H., van Eeten, Y.J., Coenen, A.M., 2004. Effects of diazepam and zolpidem on EEG beta frequencies are behaviour-specific in rats. Neuropharmacology 47, 163e174.

79. Videman, M., Tokariev, A., Saikkonen, H., Stjerna, S., Heiskala, H., Mantere, O., & Vanhatalo, S., 2016. Newborn Brain Function

Is Affected by Fetal Exposure to Maternal Serotonin Reuptake Inhibitors., Cerebral Cortex, bhw153.doi:10.1093/cercor/bhw153.

80. Viscardi, A.V.; Hunniford, M.; Lawlis, P.; Leach, M.; Turner, P.V. Development of a Piglet Grimace Scale to Evaluate Piglet Pain

81. Using Facial Expressions Following Castration and Tail Docking: A Pilot Study. Front. Vet. Sci., 2017, 4, 51.

82. Walker DW., Zornetzer S., 1974. Alcohol withdrawal in mice: Electroencephalographic and behavioral correlates. Electroencephalography and Clinical Neurology., 36:233–243.

83. Wang, Q., 2017. The recent progress in animal models of depression. Prog. Neuro-Psychopharmacol. Biol. Psychiatry 77, 99–109.

84. Ward, J., 2015. "The Student's Guide to Cognitive Neuroscience", 3rd Ed., Psychology Press, Sussex., 1–80.

85. Ward, L.M. 2003. Synchronous Neural Oscillations and Cognitive Processes. Trends Cogn. Sci., 7, 553–559.

86. Weber, F., and Dan, Y., 2016. Circuit-based interrogation of sleep control., Nature 538, 51–59. doi: 10.1038/nature19773

87. Xunxun Chu, 2019. Preliminary validation of natural depression in macaques with acute treatments of the fast-acting antidepressant ketamine, Behavioural Brain Research., 360; 60–68.

88. Yordanova, J., Banaschewski, T., Kolev, V., Woerner, W., Rothenberger, A., 2001. Abnormal early stages of task stimulus processing in children with attention-deficit hyperactivity disorder–evidence from event-related gamma oscillations. Clin. Neurophysiol., 112 (6), 1096–1108.

89. Zeng, L. H., Xu, L., Gutmann, D. H., Wong, M., 2008. Rapamycin prevents epilepsy in a mouse model of tuberous sclerosis complex., Ann. Neurol. 63, 444e453.

Optimization of Turning Parameters using RSM During Turning of AISI H11 with Dimple Textured Uncoated Carbide Tool

Chetan Darshan

ABSTRACT

In this study, an attempt is made to understand the performance of dimple textured uncoated carbide cutting tool during turning of AISI H11 hot die steel in dry environment. Response surface methodology (RSM) was adopted to evaluate the effect of turning process parameters (cutting speed 80-120 m/min, feed rate 0.16-0.32 mm/rev and depth of cut 0.2 -0.5 mm) on tool flank wear (VB) and surface roughness (Ra). The results of the experimental runs are examined using ANOVA and variable interaction plots.

Flank wear initially less at lower cutting speed of 80 m/min but as the speed increases wear on flank increases with same trends of feed rate. At low feed rate of 0.16 mm/rev surface roughness is low at all cutting speeds, whereas with increase in feed rate deteriorate the surface quality. Similarly, with 0.2 mm depth of cut Ra is 2.23 μm and with increase in depth of cut value Ra approaches 2.98 μm. Optimization and modelling was conducted to minimize wear and roughness using 5% error.

Keywords: textured tool, RSM, surface roughness, tool wear.

Classification: DDC Code: 523.1 LCC Code: QB982

Language: English

Optimization of Turning Parameters using RSM During Turning of AISI H11 with Dimple Textured Uncoated Carbide Tool

Chetan Darshan

ABSTRACT

In this study, an attempt is made to understand the performance of dimple textured uncoated carbide cutting tool during turning of AISI H11 hot die steel in dry environment. Response surface methodology (RSM) was adopted to evaluate the effect of turning process parameters (cutting speed 80-120 m/min, feed rate 0.16-0.32 mm/rev and depth of cut 0.2 -0.5 mm) on tool flank wear (VB) and surface roughness (Ra). The results of the experimental runs are examined using ANOVA and variable interaction plots.

Flank wear initially less at lower cutting speed of 80 m/min but as the speed increases wear on flank increases with same trends of feed rate. At low feed rate of 0.16 mm/rev surface roughness is low at all cutting speeds, whereas with increase in feed rate deteriorate the surface quality. Similarly, with 0.2 mm depth of cut Ra is 2.23 µm and with increase in depth of cut value Ra approaches 2.98 µm. Optimization and modelling was conducted to minimize wear and roughness using 5% error.

Confirmation of the test runs shows 3.84% and 4.47% error between predicted and experimental values of VB and Ra.

Keywords: textured tool, RSM, surface roughness, tool wear.

Author: DAV Institute of Engineering & Technology, Jalandhar.

I. INTRODUCTION

Developments in the metal cutting industry are driven by the manufacturer's need to expand the performance of parts used for various applications by maintaining the environmental legislation. Extreme heat develops at cutting edge while machining "difficult-to-cut" materials, which is carried out by workpiece, tool, and coolant/lubricants. Traditionally, to dissipate heat large quantity of coolants (flooded coolants) is used to minimize friction and heat, which create difficulties in procurement, dumping, storage, and preservation. However, some disadvantages like cost, environmental impact, safety, and health hazards limit the use of flood cooling which compels industries to minimize or eliminate its use and encourage the development of new cooling/lubricating options. "Dry machining" is oldest, most environmentally friendly options, but absence of cutting fluid leads to heat generation, adhesion, poor chip evacuation, and increase friction at the cutting zone. Dry machining is found to lead to poor results with rough surface on products, whereas flood cooling leads to economic, environmental, and health challenges.

Worldwide manufacturers are actively seeking cost-effective alternatives to produce satisfactory quality components which are accepted globally.

To promote the metal cutting industry and creating new opportunities, technology plays an important role. Turning at one time is based on the skills of the operator and still important, so to be competitive it is necessary to adopt and implement modern and cost-efficient manufacturing techniques (Soroka, 2003).

Materials used extensively in aerospace, food, and the nuclear industry have great-strength and wear-resistance are "difficult-to-machine" due to thermo-physical stresses at the edge of cutting tool (Sharma, Dogra and Suri, 2008). The degradation of the surface finish is closely associated with wear growth. Different

London Journal of Engineering Research

researchers working on enhancing tool life during conventional turning; otherwise, tool failure refers to the damage that is so severe to remove material from the workpiece due to its vulnerability to changes in cutting conditions (Sharma, Dogra and Suri, 2009). Tool-workpiece friction and heat generation at cutting area are prevalent challenges in turning, reducing life of tool and compromising the quality of surface during turning operation.

Due to unusual properties of "difficult-to-machine" materials, such as low conductivity to heat, great-strength at eminent temperatures, and wear-resistance and corrosion generate heat and produce negative effects (Zhang, Li and Wang, 2012). Enormous generation of heat (indicated in Fig. 1.1) at the cutting zone while turning "difficult-to-cut" materials, is due to plastic deformation because of chip formation and friction between the tool-work-piece and tool-chip. Dissipation of heat is dependent on geometry of tool, its heat conductivity, and cooling techniques (Shokrani, Dhokia and Newman, 2012).
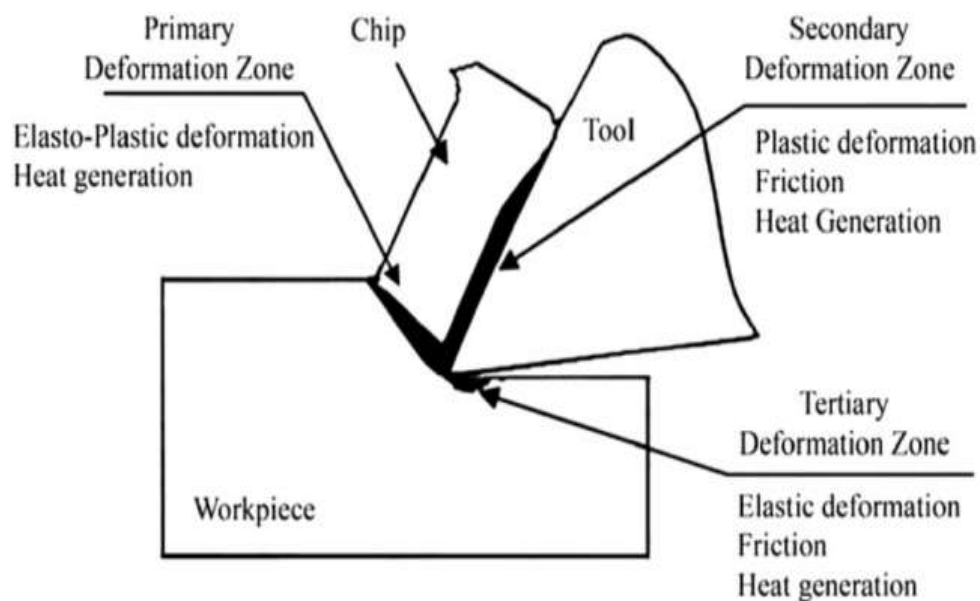
Figure 1.1: Heat generation at cutting zone (Abukhshim, Mativenga and Sheikh, 2006)

Surface topography moderation of cutting tools using textures has been an innovative/ecological method, which helps to improve tribological conditions of sliding surfaces relative to each other, and the addition of solid lubricant in the pockets generated on the tool makes dry machining environmental friendly (Sharma and Pandey, 2016).

Dry machining with surface texturing tends to be the most suitable solution for sustainable machining. But for hard materials, high-temperature gradient at cutting zone necessitates the use of traditional flood cooling, which makes the process harmful for ecological considerations (Mosarof *et al.*, 2016).

1.1 Dry Machining

Dry machining is an eco-friendly approach and it will be mandatory for the industries in the coming future to enforce regulations of environment sustainability for occupational safety and health standards (Klocke, F., & Eisenblätter, 1997).

Dry turning/machining offers pollution-free atmosphere (or water); no swarf residues that are measured by decreased disposal and cleaning costs; no health hazards; no skin and allergy (Sreejith and Ngoi, 2000). Dry machining helps to create an environmentally friendly image, reduce costs, and improve work satisfaction in workers (Figure 1.2).

Figure 1.2: Dry Machining Advantages (Ghosh and Rao, 2015)

The major issues during dry machining include overheating, enhanced abrasion, diffusion and oxidation of the tool material. However, a significant amount of heat inhibits near tolerances and its surface is subjected to metallurgical damage (Debnath, Reddy and Yi, 2014).

Dry hard turning of difficult-to-machine materials would not be feasible without the selection of appropriate tool material. Costly, CBN (cubic boron nitride) tools are widely applied to machine high hardness and thermal conductivity materials, since these are second toughest tool material after diamond. Various merits or demerits of dry hard turning are discussed in Table 1.1. The cost of the CBN tool is high, but tool wear is low in comparison to other tool materials (Kundrák *et al.*, 2006). Cemented carbide tools have been developed over time and still to be primarily used to machine Ni-alloys, particularly Inconel-718.

Conversely, with the increase demand for high MRR and higher surface quality, machining at high speed was adopted and usage of cemented carbide tools became more complex (Dudzinski *et al.*, 2004). For dry turning of Inconel-718, cutting tool material must meet the following requirements (Dudzinski *et al.*, 2004):

1. Adequate stability at high temperatures
2. Superior thermal shock resistance
3. Superior strength and toughness
4. High hot hardness
5. Excellent resistance to wear

Optimization of Turning Parameters using RSM During Turning of AISI H11 with Dimple Textured Uncoated Carbide Tool

Table 1.1: Merits and Demerits of Dry Hard Turning

Merits	Demerits
▪ Non-pollution of the environment or water, thereby reducing the health risk, especially to the skin and respiratory system ▪ No lubricant stain on machined parts that reduces or avoids the cost of cleaning and energy consumption. ▪ No lubricant residue on extracted chips reduces the cost of disposal and energy consumption associated	▪ Overheating of cutting tool ▪ High friction due to softening of tool base material. ▪ Rapid tool wear due to abrasion, diffusion, and oxidation. ▪ Damage workpiece surface due to a large amount of heat accumulated in cutting area. ▪ Formation of chip, deteriorate surface quality

1.2 Textures Engraved on Tool Surface

"Surface structuring or surface texturing on the cutting tool is an innovative strategy for sustainable metal cutting. Surface texturing is a term that refers to the process of altering the topography of a surface to enhance tribological efficiency of contact surfaces"(Fatima and Mativenga, 2013; Ghosh and Rao, 2015). In the last decade, textures on surface has been the feasible option in surface engineering, leading to considerable increments in load carrying capacity, wear, strength, friction coefficient, etc. of tribo-mechanical components (Etsion, 2005). The surface texture reduces the friction coefficient, cutting forces and sticking between the tool-chip interface (Jianxin *et al.*, 2012). Different researchers have graved various textures for this reason on tool inserts (Ghosh and Rao, 2015).

Metal cutting processes are now carried out at high speeds to ensure optimum efficiency, thanks to the advancement of modern engineering technologies. In the era of automation, long continuous chips produced at high cutting rates have become a challenge for industry. Textures on tool surface helps to control contact because their length of contact is shorter than conventional contact length of chip (Chao and Trigger, 1959).

Surface textures are generated by a variety of advanced manufacturing techniques, which include; micro-wire cut "electron discharge machining" (EDM), "Focused ion beam" (FIB) machining (Tseng, 2004), and photolithography, "reactive ion etching" method (RIE), laser technology, and so forth (Pettersson and Jacobson, 2003). Texture geometries such as micro-holes, linear, circular, square, and wavy indentations, were developed on tool surfaces and its application improves the cutting tool tribological performance (Etsion, 2005).

II. LITERATURE

Nowadays, the tendency is toward high-quality, cheap, and small-batch sizes. To compete with countries having structure of low-wage in manufacturing industry, it is vital to innovate techniques that contribute to the improvement of the manufacturing sector's level, with a beginning to witness technical improvements in the field of hard turning (Soroka, 2003). Generally, when the hardness of material is more than 45 HRC, then it is called hard turning (Pavel *et al.*, no date). While it may not remove the requirement of grinding, it may relieve the load on costly grinders for the specified application (König, Berktold and Koch, 1993; Chou, Evans and Barash, 2003).

During cutting of metal, there is maximum conversion of energy into heat. Friction inside tool-chip interface and in the workpiece-tool interaction zone generates extra heat at cutting region. The temperature due to friction and plastic deformation at the cutting zone is reached upto 1700°C. During machining 10-20% heat is taken up by tool and rest of 80-90% is transferred to chip (Budak *et al.,* 2010). Heating the tool and workpiece is excessive and also raises their temperature and distortion in the cutting tool (Motorcu *et al.,* 2016).

To overcome these problems of dry machining, sustainable techniques are developed like; a new class of tools, texturing on rake surface of tool,

improved tool geometry, and coatings are applied on tools. From all of the above, surface texturing is an environment-friendly method for tribological characteristics improvement.

"Tribology is the study of friction, wear and lubrication of the surfaces in relative motion" (Ian Hutchings, 2017). Lubrication/Cooling capabilities and tribological properties are improved as observed from literature with the help of micro-scale surface textures on cutting tools which also helps to reduce adhesion (Pettersson and Jacobson, 2003; Wakuda *et al.*, 2003; Etsion, 2005; Kovalchenko *et al.*, 2005).

Therefore, cutting tool surface texturing is a method that improves friction and lubrication during the interaction of tool and chip. Surface texture minimizes the friction by shortening the duration of contact of chip with tool (Enomoto and Sugihara, 2010; Chang *et al.*, 2011; Enomotoa and Sugihara, 2011). When texture surface chip-tool friction is reduced and the wear debris that forms from this is confined in the cavity owing to textures on the surface (Blatter *et al.*, 1999; Costa and Hutchings, 2009). During the turning of materials hard to machine, a comparative examination of textured and conventional cutting tools was done. Textured tools utilized in the turning process, helps to reduce friction, heat generation, and thus wear, which helps to improve energy efficiency, product quality, and tool life (Ling *et al.*, 2013)

The textures orientation at the cutting edge has been demonstrated to increase or decrease cutting performance, several studies have examined this in terms of sliding contacts. The tribological performance of parallel direction, perpendicular direction, and at a 45° angle to the sliding direction was tested (Pettersson and Jacobson, 2004); and found that orientation modification helps pressure accumulation due to textures; which disrupt surface roughness.

It is observed that perpendicular texture displayed more extraordinary film thickness under higher loads, whereas narrower parallel grooves exhibited a flow-direction because the lubricant may be directed away from contact in a parallel groove and so reduces the thickness of the film and tribology (Costa and Hutchings, 2007). The angle of textures was essential since they alter the lubricant's capacity to capture wear particles (Zhan and Yang, 2012). The foregoing tests show that textures must be oriented towards the sliding direction since it has a direct effect on the texture mechanism which promotes the tribological performance on a contact surfaces. For the building grooves in parallel on the rake tool face (known as textured tool), EDM has been used (Kim *et al.*, 2015) and evaluated its influence on the cuts in comparison with conventional tool.

Some researchers have discriminate textures (Fig. 2.1,showing perpendicular shape, parallel shape, and cross patterns) to chip flow direction using femtosecond laser on WC inserts (Kawasegi *et al.*, 2009).
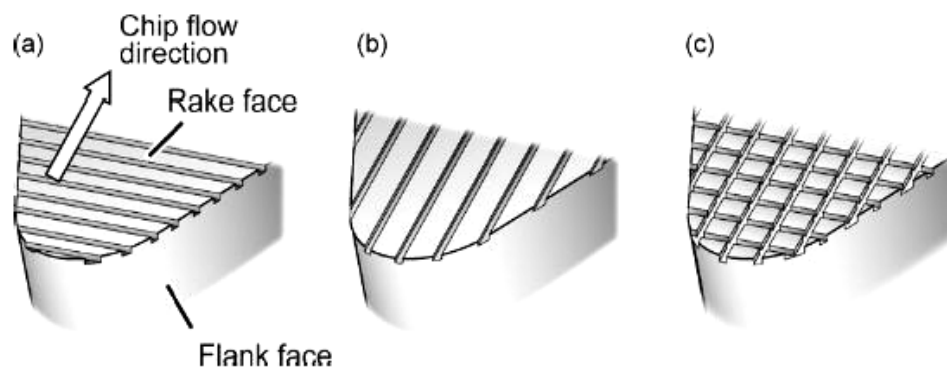
Figure 2.1: Texture on Cutting Tool According to Direction of Chip Flow (A) Perpendicular Shape (B) Parallel Shape (C) Cross Texture (Kawasegi Et al., 2009)

Wear resistance of tool is found to increased greatly in comparison to conventional insert while machining carbon steel with four kinds of textured tool because this micro-grooved surface collects the wear particles created by wear mechanisms (Enomoto and Sugihara, 2010).

Four varieties (perpendicular, parallel, square-shaped pits and dots) as depicted in Fig.

2.2 were produced in the same way. Micro-scale textures in orthogonal and diagonal sites showing that using rake and flank face grooves decreases tool wear as compared with ordinary tools (Xie *et al.*, 2012). Diagonal micro-sites reduce wear of tool by 6.7% and increase heat dissipation rate in the cutting are due to texture orientation to the chip flow direction.
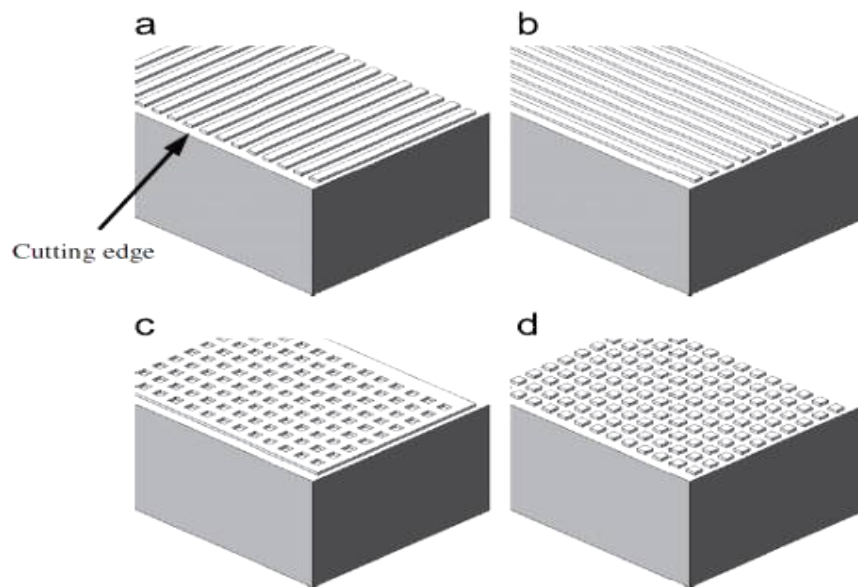
Figure 2.2: Texture Types on Tool Rake Surface (A) Perpendicular Type (B) Parallel Type (C) Pit Type and (D) Dot Type. (Obikawa Et al., 2011)

Advantages of micro/ nano-textures

1. Textures on the cutting tool help to improve machinability by lowering friction, but it depends upon the shape and size of the textures. Reduction in friction is achieved by micro/nano-scale textures as reported with the literature.
2. Reduced friction results in decreased wear, cutting forces, and chip adhesion during the cutting action.
3. Cutting tool textures aid in the retention of coolant/lubricant at the tool-chip contact, providing lubricating and cooling benefits.
4. It also reduces plowing wear by removing wear debris, which causes abrasive wear.
5. Textures serve as reservoirs for both liquid and solid lubricants, resulting in the formation of a self-lubricating barrier at the tool-chip interface. This technique is advantageous for solid lubricants because it

extends the tool life and improves the surface quality of textured tools.

III. EXPERIMENTAL SETUP

3.1 Work Piece Material

Commercially available, round bars of AISI H11-hot die steel (with axial cutting length 200 mm and diameter ϕ 22 mm) were selected as workpiece materials for tuning tests material. Composition and mechanical characteristics of AISI H11 hot die steel are given in Table 3.1 and Table 3.2.

Table 3.1: Chemical Composition of AISI-H11 (Hot Die Steel) in Wt. %

C	Si	Mn	P	S	Cr	Mo	V
0.33	0.9	0.29	0.03	0.02	5.1	1.2	0.34

Table 3.2: Mechanical Characteristics of AISI-H11 (Hot Die Steel) at Nominal Ambient-Temperature
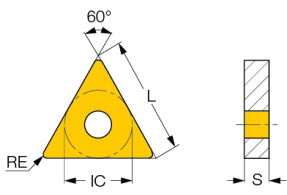
Tesile Strength (MPa)	Yield Strength (MPa)	Young modulus (MPa)	Density (g/cm³)	Melting Range (°C)	Hardness, Brinell HB	Thermal Conductivity (W/mK)
1590	1380	215×10^3	8.19	1345-1427	195	42.2

3.2 Cutting Tool Material

Cutting tool material selected for the turning tests was uncoated cemented carbide tool; ISO designation - TNMA 160408-THMF (provided by M/s Kennametal India Limited) having specifications shown in Table 3.3. The name of the tool holder was WTJNR1616H16. It was used to rigidly mount the tool mentioned above and had a tool cutting edge angle of 93°.

Table 3.3: Cutting Insert Specifications

Cutting insert	Type	Insert Geometry	Insert dimensions (mm)				No. of Edges
			L	IC	R_e	S	
	TNMA		16.50	9.52	0.80	4.76	6

Uncoated cemented carbide tool with texture on the rake face is utilized in comparison to costly CBN tools for turning "difficult-to-machine" materials. The tool holder (WTJNR1616H16) and cutting insert on clamping, gave approach angle (93°), clearance angle (6°), rake angle (-6°) and nose radius (0.80 mm). The dimensions of tool holder (in mm) are given in Table 3.4.

Table 3.4: Tool Holder Dimensions

Tool Holder	Dimensions (in mm)					
WTJNR1616	H	B	LF	LH	HF	WF
H16	20	20	125	125	25	25

3.3 Fabrication of Surface Texture on Rake Face (Dimple Shape)

In general, the several "micro-machining" techniques for removing materials, such as 'micro-grinding', 'micro-EDM', 'femtosecond laser' and 'fibre laser' have been used.
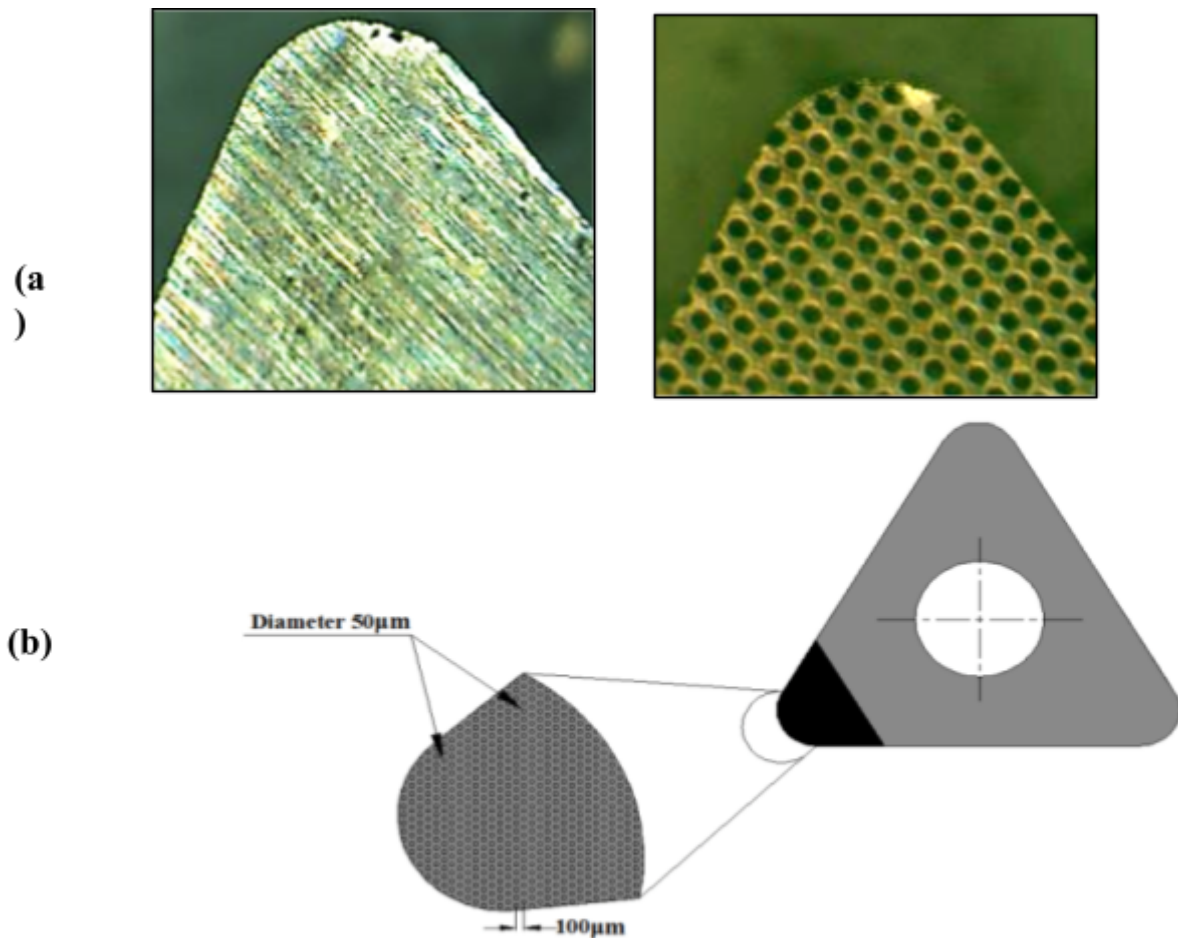
Figure STYLEREF 1 \s 3.1 Optical microscope image of **(a)** Non-textured (NT) tool and textured tool (TT) **(b)** CAD model textured tool

Dimple-shaped texture with 50 μm diameter and 100 μm special distance, as illustrated in Fig. 3.1 a,b, is taken into consideration and is modelled using CAD software. The CAD model was then exported to appropriate interface for fabricating texture on tool rake surface. A "multidiode pump fibre laser" (LM-487-A-22-SD6-UX-M30-M) was applied on uncoated carbide tool's rake surface, the array of dimple texture is taken zigzag and the direction parallel to cutting edge was fabricated.

The conventional insert with non-textured and dimple-textured pictures was measured by optical microscope and is displayed in Fig. 3.1 a, b.

3.4   Machine and Measuring Equipment

The turning runs were conducted on convention lathe HMT, India, model: high- speed precision lathe NH 22 and for tool flank wear and surface roughness   measurement Metzer toolmaker's microscope Surf Test SJ-201 analyzer are utilized.

To measure the cutting forces during cutting a strain gauge based digital lathe dynamometer supplied by RMS controls, India was used during experimentation. The specifications of cutting force dynamometer is given in Table 3.5. "Scanning electron microscopy" was used to characterize the wear of worn-out cutting inserts.

The SEM/EDAX equipment is shown in Figure 3.6 with the following specifications, associated with two computer interface for wear and elemental analysis, respectively.

Table 3.5: Specifications of Digital Lathe Dynamometer

Make	RMS Controls, India
Axis	3 axis- X, Y, Z
Sensor	500.0 kgf
Range	0.1 kgf
Resolution	0.05 % Full scale
Accuracy	0.05 %
Linearity	Front side push button switch
Zero/Tare	230 V AC
Power supply	Table
Model	Top

Table 3.6: Specification of "Scanning Electron Microscope" (SEM)

Make	JEOL, Japan
Model	JSM-6510LV
Maximum magnification	5X to 300,000X
Resolution	3 nm
Operating voltage	0.5 KV to 30 KV
Maximum specimen	150 mm diameter
Objective lens	Super conical

IV. MODELING OF FLANK WEAR AND SURFACE ROUGHNESS

To generate models for response factors, i.e., tool flank wear and surface roughness, an entire set of 20 experiments obtained through RSM based on CCFC (central composite face-centered) design have been conducted. The input turning parameters viz. cutting speed, feed rate, and depth of cut were varied over 3 levels, whereas the tool geometry and texture on the rake surface were kept constant for each experiment. The new cutting edge of the insert was used to conduct each turning test. CCFC experimental layout, along with results obtained for output responses, i.e., tool flank wear (VB) and surface roughness (Ra), is shown in Table 4.1.

In order to build their respective models in terms of input factors, the output responses were examined using RSM. The quadratic model was presented the best fit for both output factors, whereas cubic models had been aliased, in Table 4.2 and Table 4.3.

The recommended quadratic models' R-Squared (R^2) values were the greatest (except the aliased one), while their associated PRESS values remain lowest, indicating quadratic model's superiority over other source models.

Table 4.1: CCFC Experimental Layout with Results

Exp. No	Cutting speed: Vc (m/min.)	Feed rate: f (mm/rev)	Depth of cut: d (mm)	Flank wear: VB (mm)	Surface roughness: Ra (μm)
1	130	0.24	0.35	2.81	1.84
2	180	0.16	0.2	2.65	1.78
3	180	0.32	0.2	3.11	2.12
4	80	0.16	0.2	1.74	1.86
5	80	0.32	0.2	2.19	2.6
6	80	0.16	0.5	1.81	2.23
7	80	0.24	0.35	2	2.34
8	80	0.32	0.5	2.21	2.98
9	130	0.24	0.35	2.54	2.02
10	130	0.24	0.5	2.65	2.21
11	130	0.24	0.35	2.77	1.99
12	130	0.24	0.35	2.54	2.18
13	130	0.24	0.2	2.64	1.87
14	130	0.32	0.35	2.64	2.24
15	180	0.16	0.5	2.97	2.04
16	130	0.24	0.35	2.74	1.94
17	180	0.24	0.35	3.07	2.18
18	130	0.16	0.35	2.3	1.78
19	130	0.24	0.35	2.62	1.96
20	180	0.32	0.5	3.33	2.44

Table 4.2: Comparison Models for Tool Flank Wear (VB)

Source models	R^2	PRESS values	Remarks
Linear	0.9281	0.3621	
2FI	0.9364	0.6941	
Quadratic	0.9707	0.2568	Suggested
Cubic	0.9743	19.70	Aliased

Table 4.3: Comparison Models for Surface Roughness (Ra)

Source models	R^2	PRESS values	Remarks
Linear	0.7169	0.8139	
2FI	0.7610	2.06	
Quadratic	0.9099	0.2107	Suggested
Cubic	0.9613	3.27	Aliased

4.1 ANOVA Analysis

The ANOVA test was used to determine the statistical significance of models and input variables produced by RSM. Findings through ANOVA for VB and Ra models are shown in Table 4.4 and Table 4.6 respectively. The importance of RSM models and input variables may be determined by examining their associated p-value (Prob>F). If the p-value < 0.05 (Prob>F, at 95% confidence level), the contribution of parameters is considered significant. Using the ANOVA test, it was determined that models for VB and Ra are fitted and significant statistically. ANOVA findings indicate that A, B, C, AB, AC, BC, A², B², and C², are all statistically significant variables for both output responses. Lack of fit: F-test was used to determine how well the generated response models fit the input data. F-values (i.e., the ratio between mean square lack of fit and pure error mean square) for lack of fit test were found as 0.3969, and 0.2749 for VB and Ra models, respectively and their associated p-values (>0.05)

representing lack of fitness, as strongly sought model adequacy, are statistical insignificant compared to pure error. The variation coefficient (C.V. = (Std. Dev. / mean) × 100) provides an estimate of the pure error of the models' VB and Ra. The summary of model statistics for output response models (Table 4.5 and Table 4.7), indicating a strong signal for dependability of machine and accuracy of the model, indicate a low value of C.V. for both models (<10%).

Likewise,; R^2 or R-squared = 1- (residual sum of squares / total sum of squares) was higher than 0.85, for both models, which confirmed furthermore the accuracy of the models that were fitted with regard to the projection of capability of response parameters. The values of output responses that are predicted by the adjusted R^2 and R^2 indicate excellent interactions. In addition, adequate precision (AP: signal/noise ratio) > 4, shows the validity of the models for future predictions for both models. Furthermore, the lowest press values (predicted residuals error sum of squares): 0.2568 and 0.2107, shows quadratic models for output responses are best fit models for the test findings.

Table 4.4: ANOVA Results for Tool Flank Wear (VB)

Source	Sum of Squares	DF*	Mean Square	F value	p-value Prob>F	Remarks
Model	3.27	9	0.3635	36.76	< 0.0001	significant
A-Cutting speed (*Vc*)	2.68	1	2.68	271.31	< 0.0001	
B-Feed rate (*f*)	0.404	1	0.404	40.85	< 0.0001	
C-Depth of cut (*d*)	0.041	1	0.041	4.14	0.0692	
AB	0.0001	1	0.0001	0.0114	0.9172	
AC	0.0253	1	0.0253	2.56	0.1407	
BC	0.0028	1	0.0028	0.2844	0.6055	
A^2	0.0118	1	0.0118	1.19	0.3007	
B^2	0.0468	1	0.0468	4.73	0.0547	
C^2	0.0055	1	0.0055	0.5517	0.4747	
Residual	0.0989	10	0.0099			
Lack of Fit	0.0281	5	0.0056	0.3969	0.8333	not significant
Pure Error	0.0708	5	0.0142			
Cor Total	3.37	19				

*Degrees of Freedom

Table 4.5: Tool Flank Wear- VB Model Statistics

Std. Deviation	0.0994		R^2	0.9707
Mean	2.57		Adjusted R^2	0.9443
C.V. %	3.87		Predicted R^2	0.9238
PRESS	0.2568		Adeq Precision	22.2693

Table 4.6: ANOVA Results for Surface Roughness (Ra)

Source	Sum of Squares	DF*	Mean Square	F value	p-value Prob>F	Remarks
Model	1.61142	9	0.179	22.332	0.00002	significant
A-Cutting speed (*Vc*)	0.21025	1	0.210	26.224	0.00045	
B-Feed rate (*f*)	0.72361	1	0.724	90.253	0.00000	
C-Depth of cut (*d*)	0.27889	1	0.279	34.785	0.00015	

AB	0.07031	1	0.070	8.770	0.01425	
AC	0.00361	1	0.004	0.451	0.51727	
BC	0.00061	1	0.001	0.076	0.78787	
A²	0.16324	1	0.163	20.360	0.00112	
B²	0.00011	1	0.000	0.014	0.90852	
C²	0.00154	1	0.002	0.192	0.67087	
Residual	0.08018	10	0.008			
Lack of Fit	0.01729	5	0.003	0.275	0.90858	not significant
Pure Error	0.06288	5	0.013			
Cor Total	1.69160	19				

Table 4.7: Surface Roughness- Ra Model Statistics

Std. Deviation	0.0895		R^2	0.9526
Mean	2.13		Adjusted R^2	0.9099
C.V. %	4.20		Predicted R^2	0.8755
PRESS	0.2107		Adeq Precision	19.6007

To create a connection between response variables and input turning factors, multiple regression analysis was used to produce output response (VB and Ra) mathematical models. Table 4.8 lists empirical models for output responses.

Table 4.8: Empirical Model Equations

Sr. No.	Response Factors	Empirical Model Equations (In Terms of Actual Factors)
1	VB	$-0.650240 + 0.014767 * Vc + 12.96534 * f - 1.55919 * d - 0.000938 * Vc * f + 0.007500 * Vc * d - 1.56250 * f * d - 0.000026 * (Vc)^2 - 20.38352 * (f)^2 + 1.97980 * (d)^2$
2	Ra	$2.09936 - 0.021622 * Vc + 6.63144 * f + 0.571313 * d - 0.023438 * Vc * f - 0.002833 * Vc * d + 0.729167 * f * d + 0.000097 * (Vc)^2 - 0.994318 * (f)^2 + 1.05051 * (d)^2$

To check the accuracy of developed models for VB and Ra, shown in Table 8.8, the values of VB and Ra have been calculated from these regression equations for a different combination of input parameters, as reported in Table 4.1. The anticipated model values (for VB and Ra) are compared with the experimentally examined values. Figures 4.1 and 4.2 demonstrate that the anticipated and empirically observed values (for VB and Ra) are very congruent.
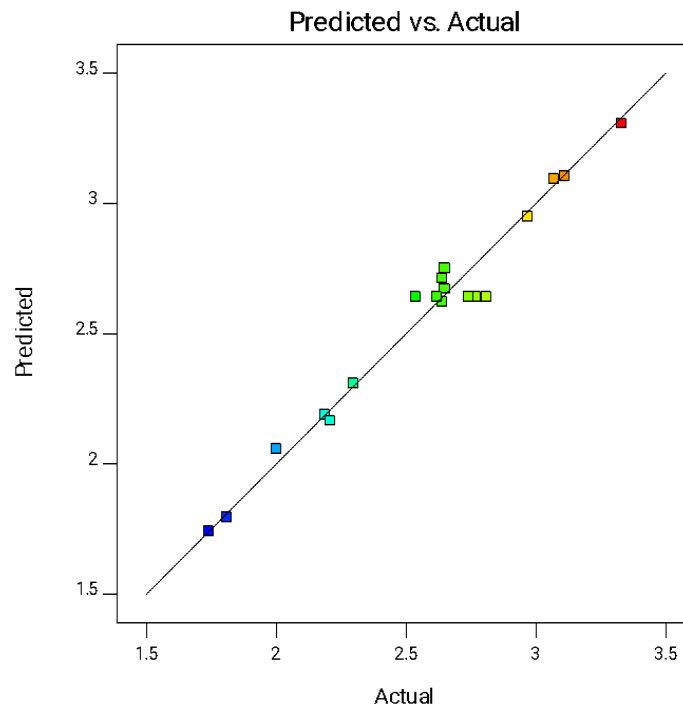
Figure 4.1: Predicted and Actual Comparative Values of VB
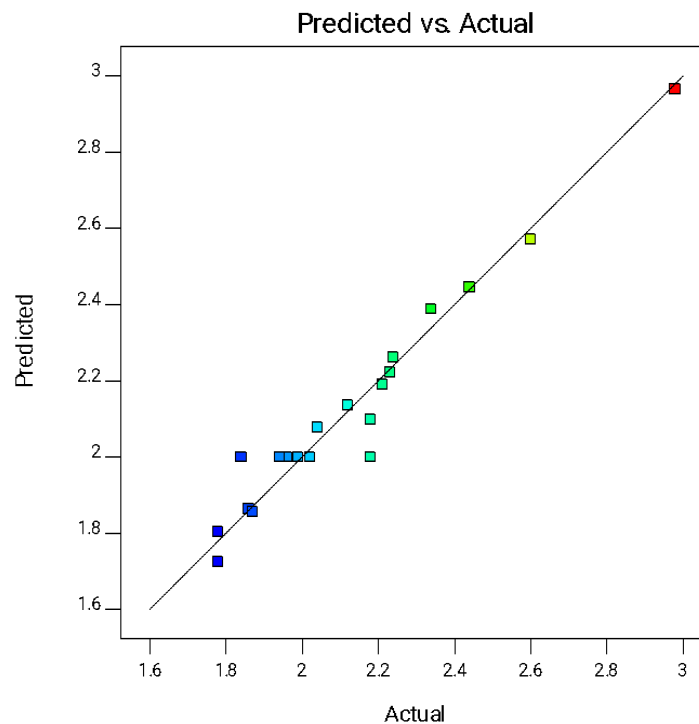
Figure 4.2: Predicted and Actual Comparative Values of Ra

4.2   Influence of Input Parameters on Tool Wear and Surface Roughness

A statistically significant model consisting of the feed rate (f) and cutting speed-depth of cut interaction (Vc-d) for flank wear of tool was used. Flank wear (VB) has been significantly varied with a change of speed. However, as is apparent from Fig 4.3, the wear of tool somewhat changes with feed rate.
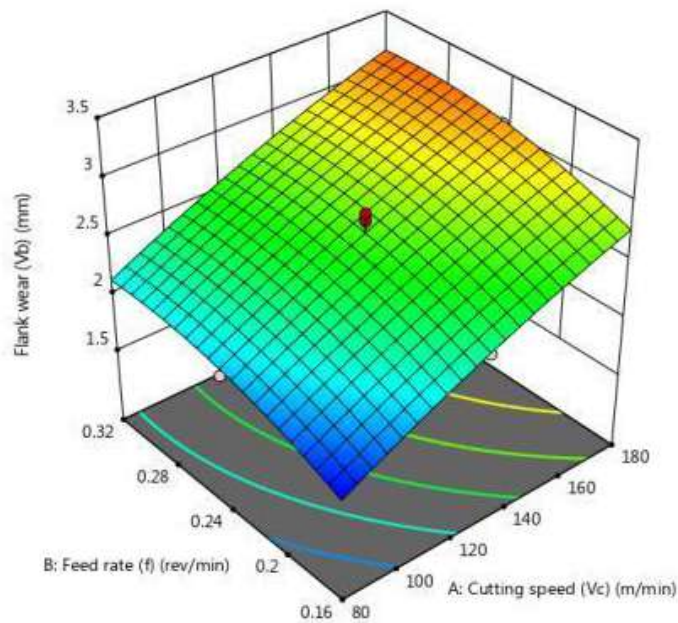
Figure 4.3: Effect of Feed Rate and Cutting Speed on VB

Wear at tool is minimal at lower cutting speed, but rises with cutting speed increases, for all feed rate range from minimum 80 m/min.., and then increases quickly with an increase in cutting speed. On the other side, tool wear is less at low feed rates, but as feed rate rises, tool wear increases somewhat. Less tool wears initially with increased cutting speed and feed rate is attributable to the attachment of workpiece-chip material on flank face, as illustrated in SEM pictures of the worn-out tool for Exp. No. 9 (Fig. 4.4-b). Fig. 4.3 showed high speed and lower feed rates, accelerate wear of tool beyond the mean value would influence turning conditions, which would increase the temperature of the area to be cut and soften the adherement layer, which is detached as shown in SEM image for Exp. No. 2 (Fig 4.4-a).

Fig. 4.3 reported high wear at flan with higher feed rate/ speed. Initially, the tool edge was protected by hard particle and rake face textures, which limits chip tool contact, resulting in less tool flank wear, as the speed and feed rate rises, temperature between tool-chip interfaces becomes dominating factor. At high speed cutting, the friction rises due to uneven contact with a chip-tool, which causes the protective layer to be removed, i.e. adhesive wear. Furthermore, due to the high temperature during cutting, the bonds between tool particles are weakened by the severe diffusion between the work material and tool. The hard particles are thus removed from the tool and wear is thereby enhanced. The tool flank wear (VB) rises with an increase in feed rate, but above the mean value, the VB increases quickly. A reduction in tool flank wear was seen with a combination of low cutting speed and low feed.
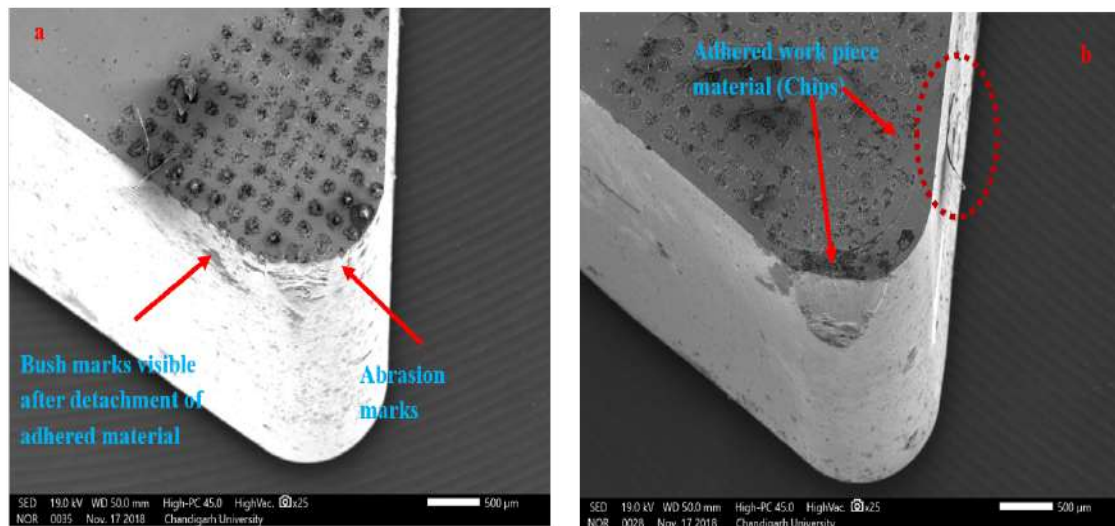
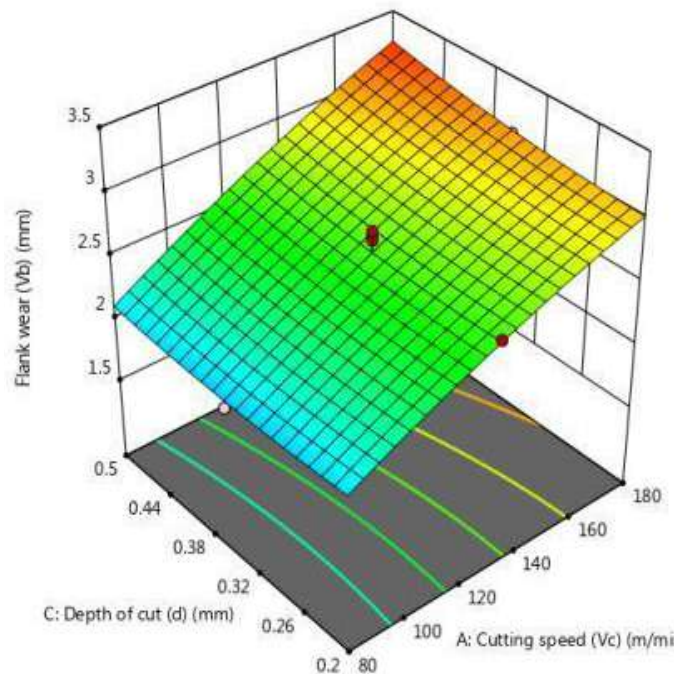*Figure 4.4:* SEM Images of Worn-Out Cutting Inserts

Figure 4.5: Effect of Cutting Speed and Depth of Cut on VB

The wear at the tool flank (VB) changes significantly when the depth cuts and speed range are low to moderate. However, the wear increases rapidly, as seen in Fig. 4.5. Fig. 4.5 showed depth cuts has marginal impact on wear of tool.
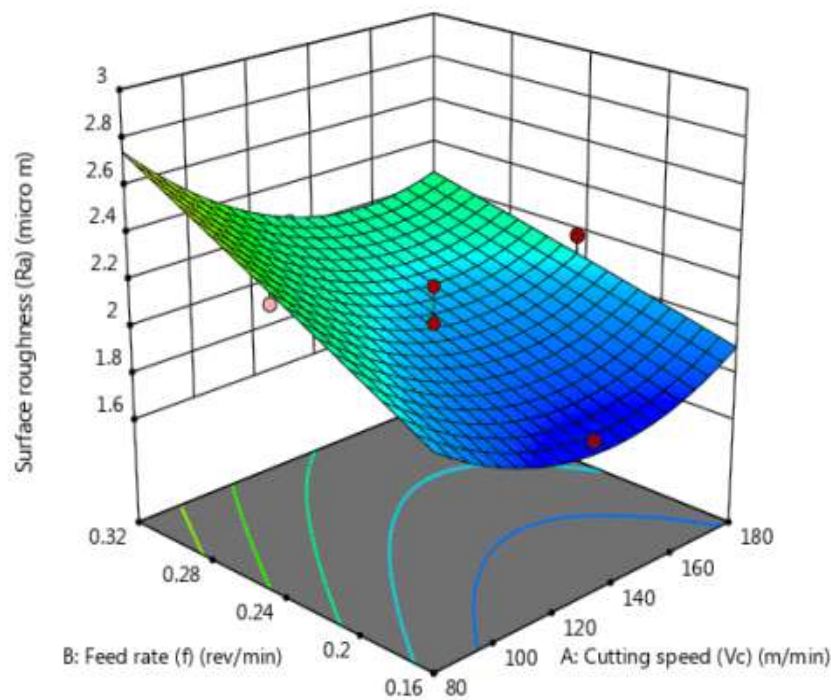
Figure 4.6: Effect of Feed Rate and Cutting Speed on Ra

Figure 4.6 illustrates the feed rate-cutting speed impact roughness (Ra), roughness of surface reduces at low feed rate, i.e., 0.16 mm/rev., with a cutting speed increase of 80 m/min.-180 m/min.

Figure 4.7: Effect of Depth of Cut and Cutting Speed on Ra

But, roughness of surface rises to 2.7 μm at high level of feed rate (0.32 mm/rev.). At a cutting speed of 80 m/min., roughness of surface (Ra) value is greater, but at 130 m/min., it drops to 1.78 μm, followed by a little higher cutting speed.

The impact of speed and cuts depth on Ra is shown in Figure 4.7. The impact was comparable

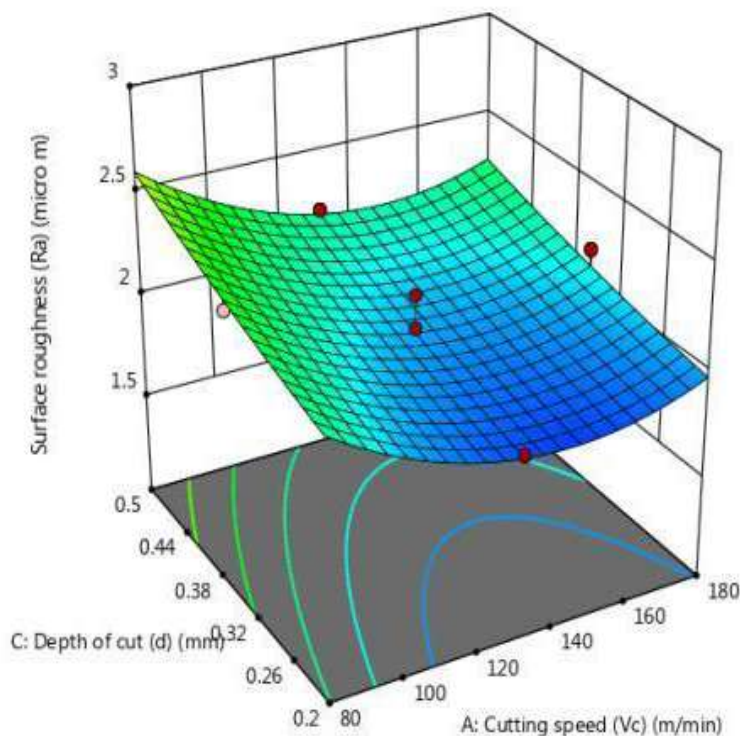to the effects of feed rate, as, at lower speed of cutting, Ra is higher, and as the speed increases, up to 130 m/min. values of Ra decreases. But with the further increment of speed of cutting does not have a noteworthy effect on Ra.

Whereas on other hand, the cuts depth (*d*) has a significant influence on roughness (Ra). At lower depth of cut (0.2 mm), surface roughness is nearly 2.23 μm, while with rise in cuts depth, roughness increases up to 2.98 μm. As illustrated in Fig. 4.7, the lowest roughness of surface was achieved by low depth of cut and speed of cutting.

4.3 Multi-Response Optimization of Turning Parameters

For optimizing turning variables for AISI H11 multi-response optimization using desirability function was employed with uncoated carbide tool to achieve minimal tool flank wear (VB) and surface roughness (Ra) using textured tools. The numerical optimization algorithm seeks a set of factors levels that simultaneously satisfies the criteria placed on each response factor with highest combined desirability. The various constraints applied throughout the optimization process are described in Table 4.9.

Table 4.9: Constraints Applied for Optimization of Turning Parameters

Constraints	Goal	Lower Limit	Upper Limit
Cutting Speed (m/min.)	is in range	80	180
Feed rate (mm/rev.)	is in range	0.16	0.32
Depth of cut (mm)	is in range	0.2	0.5
Flank wear, VB (μm)	minimize	1.74	3.33
Surface roughness, Ra (μm)	minimize	1.78	2.98

The cutting parameters were determined to be optimal as: cutting speed (*Vc* = 86.61 m/min.), feed rate (*f* = 0.16 mm/rev.) and depth of cut (*d* = 0.2 mm) with projected optimum value of VB = 1.82 μm and Ra = 1.79 μm at a desirability level of 0.967 (Table 4.10; Solution no.1).

Table 4.10: Optimization Solutions

S No.	Cutting Speed (m/min.)	Feed rate (mm/rev.)	Depth of cut (mm)	VB (μm)	Ra (μm)	Desirability	Remarks
1	86.616	0.160	0.200	1.820	1.799	0.967	Selected
2	87.054	0.160	0.200	1.824	1.795	0.967	
3	87.573	0.160	0.200	1.830	1.790	0.967	
4	85.628	0.160	0.200	1.808	1.808	0.967	
5	88.012	0.160	0.200	1.835	1.787	0.967	

4.4 Confirmation Tests

Confirmation tests (replicated thrice) have been carried out under the same experimental settings and tooling circumstances, with suggested optimal levels of machining variables. Table 4.11 demonstrates the error between the expected response and the experimental results from validating the precision of the mathematical model created for both VB and Ra during the confirmatory tests within the 95% prediction range, illustrated in Table 4.11.

Optimization of Turning Parameters using RSM During Turning of AISI H11 with Dimple Textured Uncoated Carbide Tool

Table 4.11: Results of Confirmation Tests

Response factor	Results obtained at machining parameters (86.6 m/min., 0.16mm/rev. and 0.2 mm)		
	RSM Predicted value	Experimentally observed value	Error (%)
Tool flank wear (μm)	1.82	1.89	3.84%
Surface roughness (μm)	1.79	1.87	4.47%

V. CONCLUSION

In this study mathematical models has been developed for turning AISI H11 steel using uncoated carbide textured (dimple shape) tool to analyse the effect of variation of i.e. cutting speed (V_c), feed rate (f) and cutting depth (d) on output responses viz. tool flank wear (VB) and surface roughness (Ra) using RSM. The following conclusions are derived:

a) ANOVA results reveals A, B, C, AB, AC, BC, A², B², and C², are the statistically significant parameters for both output responses i.e. tool flank wear (VB) and roughness of surface (Ra).

b) Wear of tool initially decreases to some extent with rise in cutting speed at all feed rate range at about 80 m/min., and increases quickly with cutting speed rise. Wear of tool shows similar behaviour with change in feed rate from 0.16-0.32 mm/rev. for all speed range for cutting. Maximum wear on flank of tool occurs at maximum cutting speed of 180 m/min. and maximum feed rate of 0.32 mm/rev. Wear at the tool flank (VB) significantly rises with rise in cutting depth i.e. from 0.2-0.5 mm and speed range i.e. from 80-180 m/min..

c) At low level of feed rate i.e. at 0.16 mm/rev., roughness of surface (Ra) decreases with rise in cutting speed from 80-180 m/min. However, at high value of feed rate (0.32 mm/rev.), Ra is high at low cutting speed i.e. 80 m/min.., but as the speed of cutting rises roughness of surface become stable. The value of Ra increases significantly with change in feed rate from 0.16 to 0.32 mm/rev, at range of speed. Cutting depth

also significantly affect Ra, at low cutting depth i. e. 0.2mm, Ra is 2.23 μm, whereas increase in cuts depth it rises to 2.98 μm.

d) Best value of surface quality is achieved corresponding to combination of lowest feed rate and cutting depth with highest speed of cutting.

e) The optimized machining parameters for minimizing wear of tool and roughness of surface are approaching: cutting speed (V_c = 86.61 m/min.), feed rate (f = 0.16 mm/rev.) and cutting depth (d = 0.2 mm) with predicted optimum value of VB = 1.82 μm and Ra = 1.79 μm at desirability level of 0.967.

f) Confirmation tests validate accuracy of the RSM generated models. The results show 3.84% and 4.47% error between predicted and experimental observed values of VB and Ra, respectively.

REFERENCES

1. Blatter, A. *et al.* (1999) 'Lubricated sliding performance of laser-patterned sapphire', *Wear*, 232(2), pp. 226–230. Available at: https://doi.org/10.1016/S0043-1648(99)00150-7.

2. Chang, W. *et al.* (2011) 'Investigation of microstructured milling tool for deferring tool wear', *Wear*, 271(9–10), pp. 2433–2437. Available at: https://doi.org/10.1016/j.wear.2010.12.026.

3. Chao, B. T. and Trigger, K. J. (1959) 'Controlled Contact Cutting Tools', *Journal of Engineering for Industry*, 81(2), pp. 139–147. Available at: https://doi.org/10.1115/1.4008274.

4. Chou, Y. K., Evans, C. J. and Barash, M. M. (2003) 'Experimental investigation on cubic boron nitride turning of hardened AISI 52100 steel', *Journal of Materials Processing Technology*, 134(1), pp. 1–9. Available at: https://doi.org/10.1016/S0924-0136(02)00070-5.

5. Costa, H.L. and Hutchings, I.M. (2007) 'Hydrodynamic lubrication of textured steel surfaces under reciprocating sliding conditions', *Tribology International*, 40(8), pp. 1227–1238. Available at: https://doi.org/10.1016/j.triboint.2007.01.014.

6. Costa, H. L. and Hutchings, I. M. (2009) 'Effects of die surface patterning on lubrication in strip drawing', *Journal of Materials Processing Technology*, 209(3), pp. 1175–1180. Available at: https://doi.org/10.1016/j.jmatprotec.2008.03.026.

7. Debnath, S., Reddy, M. M. and Yi, Q. S. (2014) 'Environmental friendly cutting fluids and cooling techniques in machining: A review', *Journal of Cleaner Production*, 83, pp. 33–47. Available at: https://doi.org/10.1016/j.jclepro.2014.07.071.

8. Dudzinski, D. *et al.* (2004) 'A review of developments towards dry and high speed machining of Inconel 718 alloy', *International Journal of Machine Tools and Manufacture*, 44(4), pp. 439–456. Available at: https://doi.org/10.1016/S0890-6955(03)00159-7.

9. Enomoto, T. and Sugihara, T. (2010) 'Improving anti-adhesive properties of cutting tool surfaces by nano-/micro-textures', *CIRP Annals - Manufacturing Technology*, 59(1), pp. 597–600. Available at: https://doi.org/10.1016/j.cirp.2010.03.130.

10. Enomotoa, T. and Sugihara, T. (2011) 'Improvement of anti-adhesive properties of cutting tool by nano/micro textures and its mechanism', *Procedia Engineering*, 19, pp. 100–105. Available at: https://doi.org/10.1016/j.proeng.2011.11.086.

11. Etsion, I. (2005) 'State of the art in laser surface texturing', *Journal of Tribology*, 127(1), pp. 248–253. Available at: https://doi.org/10.1115/1.1828070.

12. Fatima, A. and Mativenga, P. T. (2013) 'Assessment of tool rake surface structure geometry for enhanced contact phenomena', *International Journal of Advanced Manufacturing Technology*, 69(1–4), pp. 771–776. Available at: https://doi.org/10.1007/s00170-013-5079-6.

13. Ghosh, S. and Rao, P. V. (2015) 'Application of sustainable techniques in metal cutting for enhanced machinability : a review', *Journal of Cleaner Production* [Preprint]. Available at: https://doi.org/10.1016/j.jclepro.2015.03.039

14. Ian Hutchings, P. S. (2017) *Tribology: Friction and Wear of Engineering Materials*. Second. Edited by Butterworth-Heinemann.

15. Jianxin, D. *et al.* (2012) 'Performance of carbide tools with textured rake-face filled with solid lubricants in dry cutting processes', *International Journal of Refractory Metals and Hard Materials*, 30(1), pp. 164–172. Available at: https://doi.org/10.1016/j.ijrmhm.2011.08.002.

16. Kawasegi, N. *et al.* (2009) 'Development of cutting tools with microscale and nanoscale textures to improve frictional behavior', *Precision Engineering* [Preprint]. Available at: https://doi.org/10.1016/j.precisioneng.2008.07.005.

17. Kim, D. M. *et al.* (2015) 'Finite element modeling of hard turning process via a micro-textured tool', *The International Journal of Advanced Manufacturing Technology*, 78(9–12), pp. 1393–1405. Available at: https://doi.org/10.1007/s00170-014-6747-x.

18. Klocke, F., & Eisenblätter, G. (1997) 'Dry Cutting', *CIRP Annuals*, 46(2), pp. 519–526.

19. König, W., Berktold, A. and Koch, K.F. (1993) 'Turning versus Grinding - A Comparison of Surface Integrity Aspects and Attainable Accuracies', *CIRP Annals - Manufacturing Technology*, 42(1), pp. 39–43. Available at: https://doi.org/10.1016/S0007-8506(07)62387-7.

20. Kovalchenko, A. *et al.* (2005) 'The effect of laser surface texturing on transitions in lubrication regimes during unidirectional sliding contact', *Tribology International*, 38(3), pp. 219–225. Available at: https://doi.org/10.1016/j.triboint.2004.08.004.

London Journal of Engineering Research

21. Kundrák, J. *et al.* (2006) 'Environmentally friendly precision machining', *Materials and Manufacturing Processes*, 21(1), pp. 29–37. Available at: https://doi.org/10.1080/AMP-200060612.

22. Ling, T.D. *et al.* (2013) 'Surface texturing of drill bits for adhesion reduction and tool life enhancement', *Tribology Letters*, 52(1), pp. 113–122. Available at: https://doi.org/10.1007/s11249-013-0198-7.

23. Mosarof, M. H. *et al.* (2016) 'Surface Texture Manufacturing Techniques and Tribological Effect of Surface Texturing on Cutting Tool Performance: A Review', *Critical Reviews in Solid State and Materials Sciences*, 41(6), pp. 447–481. Available at: https://doi.org/10.1080/10408436.2016.1186597.

24. Motorcu, A. R. *et al.* (2016) 'Analysis of the cutting temperature and surface roughness during the orthogonal machining of AISI 4140 alloy steel via the taguchi method', *Materiali in Tehnologije*, 50(3), pp. 343–351. Available at: https://doi.org/10.17222/mit.2015.021.

25. Pavel, R. *et al.* (no date) 'Surface Quality and Tool Wear in Interrupted Hard Turning of 1137 Steel Shafts'.

26. Pettersson, U. and Jacobson, S. (2003) 'Influence of surface texture on boundary lubricated sliding contacts', *Tribology International*, 36(11), pp. 857–864. Available at: https://doi.org/10.1016/S0301-679X(03)00104-X.

27. Pettersson, U. and Jacobson, S. (2004) 'Friction and wear properties of micro textured DLC coated surfaces in boundary lubricated sliding', *Tribology Letters*, 17(3), pp. 553–559. Available at: https://doi.org/10.1023/B:TRIL.0000044504.76164.4e.

28. Sharma, V. and Pandey, P.M. (2016) 'Recent advances in turning with textured cutting tools: A review', *Journal of Cleaner Production*, 137, pp. 701–715. Available at: https://doi.org/10.1016/j.jclepro.2016.07.138.

29. Sharma, V. S., Dogra, M. and Suri, N. M. (2008) 'Advances in the turning process for productivity improvement-A review', *Proceedings of the Institution of Mechanical Engineers, Part B: Journal of Engineering Manufacture*, 222(11), pp. 1417–1442. Available at: https://doi.org/10.1243/09544054JEM1199.

30. Sharma, V. S., Dogra, M. and Suri, N. M. (2009) 'Cooling techniques for improved productivity in turning', *International Journal of Machine Tools and Manufacture*, 49(6), pp. 435–453. Available at: https://doi.org/10.1016/j.ijmachtools.2008.12.010.

31. Shokrani, A., Dhokia, V. and Newman, S.T. (2012) 'Environmentally conscious machining of difficult-to-machine materials with regard to cutting fluids', *International Journal of Machine Tools and Manufacture*, 57, pp. 83–101. Available at: https://doi.org/10.1016/j.ijmachtools.2012.02.002.

32. Soroka, D.P. (2003) 'Hard Turning and the Machine Tool', pp. 1–7.

33. Sreejith, P. S. and Ngoi, B. K. A. (2000) 'Dry machining: Machining of the future', *Journal of Materials Processing Technology*, 101(1), pp. 287–291. Available at: https://doi.org/10.1016/S0924-0136(00)00445-3.

34. Tseng, A. A. (2004) 'Recent developments in micromilling using focused ion beam technology', *Journal of Micromechanics and Microengineering*, 14 (4). Available at: https://doi.org/10.1088/0960-1317/14/4/R01.

35. Wakuda, M. *et al.* (2003) 'Effect of surface texturing on friction reduction between ceramic and steel materials under lubricated sliding contact', *Wear*, 254 (3–4), pp. 356–363. Available at: https://doi.org/10.1016/S0043-1648(03)00004-8.

36. Xie, J. *et al.* (2012) 'Micro-grinding of micro-groove array on tool rake surface for dry cutting of titanium alloy', *International Journal of Precision Engineering and Manufacturing*, 13(10), pp. 1845–1852. Available at: https://doi.org/10.1007/s12541-012-0242-9.

37. Zhan, J. and Yang, M. (2012) 'Investigation on Dimples Distribution Angle in Laser Texturing of Cylinder-Piston Ring System', *Tribology Transactions*, 55(5), pp. 693–697. Available at: https://doi.org/10.1080/10402004.2012.694581.

38. Zhang, S., Li, J. F. and Wang, Y. W. (2012) 'Tool life and cutting forces in end milling Inconel 718 under dry and minimum quantity

cooling lubrication cutting conditions', *Journal of Cleaner Production* [Preprint]. Available at: https://doi.org/10.1016/j.jcl epro.2012.03.014.

Great Britain Journal Press Membership

For Authors, subscribers, Boards and organizations

Great Britain Journals Press membership is an elite community of scholars, researchers, scientists, professionals and institutions associated with all the major disciplines. Great Britain memberships are for individuals, research institutions, and universities. Authors, subscribers, Editorial Board members, Advisory Board members, and organizations are all part of member network.

Read more and apply for membership here:
https://journalspress.com/journals/membership

For Authors

For Institutions

For Subscribers

Author Membership provide access to scientific innovation, next generation tools, access to conferences/seminars/ symposiums/webinars, networking opportunities, and privileged benefits. Authors may submit research manuscript or paper without being an existing member of GBJP. Once a non-member author submits a research paper he/she becomes a part of "Provisional Author Membership".

Society flourish when two institutions Come together." Organizations, research institutes, and universities can join GBJP Subscription membershipor privileged "Fellow Membership" membership facilitating researchers to publish their work with us, become peer reviewers and join us on Advisory Board.

Subscribe to distinguished STM (scientific, technical, and medical) publisher. Subscription membership is available for individuals universities and institutions (print & online). Subscribers can access journals from our libraries, published in different formats like Printed Hardcopy, Interactive PDFs, EPUBs, eBooks, indexable documents and the author managed dynamic live web page articles, LaTeX, PDFs etc.

JOURNAL AVAILABLE IN

PRINTED VERSION, INTERACTIVE PDFS, EPUBS, EBOOKS, INDEXABLE
DOCUMENTS AND THE AUTHOR MANAGED DYNAMIC LIVE WEB PAGE
ARTICLES, LATEX, PDFS, RESTRUCTURED TEXT, TEXTILE, HTML, DOCBOOK,
MEDIAWIKI MARKUP, TWIKI MARKUP, OPML, EMACS ORG-MODE & OTHER

support@journalspress.com
www.journalspress.com

*THIS JOURNAL SUPPORT AUGMENTED REALITY APPS AND SOFTWARES